Environmental Science and Pollution Research (2024) 31:53796–53822
https://doi.org/10.1007/s11356-023-30613-6

NOVEL REMOTE SENSING TECHNOLOGIES FOR NATURAL HAZARD MANAGEMENT

A comparative study of morphometric, hydrologic, and semi-empirical methods for the prioritization of sub-watersheds against flash flood-induced landslides in a part of the Indian Himalayan Region

Sachchidanand Singh[1,2] · Mitthan Lal Kansal[1]

Received: 24 May 2023 / Accepted: 18 October 2023 / Published online: 3 November 2023

Abstract
The flash flood-induced erosion is the primary contributor to soil loss within the Indian Himalayan Region (IHR). This phenomenon is exacerbated by a confluence of factors, including extreme precipitation events, undulating topographical features, and suboptimal soil and water conservation practices. Over the past few decades, several flash flood events have led to the significant degradation of pedosphere strata, which in turn has caused landslides along with fluvial sedimentation in the IHR. Researchers have advocated morphometric, hydrologic, and semi-empirical methods for assessing flash flood-induced soil erosion in hilly watersheds. This study critically examines these methods and their applicability in the Alaknanda River basin of the Indian Himalayan Region. The entire basin is delineated into 12 sub-watersheds, and 13 morphometric parameters are analyzed for each sub-watershed. Thereafter, the ranking of sub-watersheds vulnerability is assigned using the Principal Component Analysis (PCA), compounding method (CM), Geomorphological Instantaneous Unit Hydrograph (GIUH), and Revised Universal Soil Loss Equations (RUSLE) approaches. While the CM method uses all 13 parameters, the PCA approach suggests that the first four principal components are the most important ones, accounting for approximately 89.7% of the total variance observed within the dataset. The GIUH approach highlights the hydrological response of the catchment, incorporating dynamic velocity and instantaneous peak magnifying the flash flood susceptibility, lag time, and the time to peak for each sub-watershed. The RUSLE approach incorporates mathematical equations for estimating annual soil loss utilizing rainfall-runoff erosivity, soil erodibility, topographic, cover management, and supporting practice factors. The variations in vulnerability rankings across various methods indicate that each method captures distinct aspects of the sub-watersheds. The decision-maker can use the weighted average to assign the overall vulnerability to each sub-watershed, aggregating the values from various methods. This study considers an equal weight to the morphometric, hydrological GIUH, and semi-empirical RUSLE techniques to assess the integrated ranking of various sub-watersheds. Vulnerability to flash flood-induced landslides in various sub-watersheds is categorized into three classes. Category I (high-priority) necessitates immediate erosion control measures and slope stabilization. Category II (moderate attention), where rainwater harvesting and sustainable agricultural practices are beneficial. Category III (regular monitoring) suggests periodic community-led soil assessments and afforestation. Sub-watersheds WS11, WS8, WS5, and WS12 are identified under category I, WS7, WS4, WS9, and WS6 under category II, and WS1, WS3, WS2, and WS10 under category III. The occurrence of landslides and flash-flood events and field observations validates the prioritization of sub-watersheds, indicating the need for targeted interventions and regular monitoring activities to mitigate environmental risks and safeguard surrounding ecosystems and communities.

Keywords Sub-watershed prioritization · GIUH · Principal Component Analysis · RUSLE · Flash flood-induced erosion

Introduction

The Indian Himalayan topography is prone to flash flood-induced soil erosion processes that are triggered due to extreme rainfall incidents. These incidents result in landslides and mudflows, which further cause infrastructure

Responsible Editor: Philippe Garrigues

Extended author information available on the last page of the article

failures (Pandey and Mishra 2021). Moreover, due to anthropogenic activities and climate change, the river basins in the Himalayas are becoming increasingly susceptible to soil erosions (Budakoti et al. 2019; Thakur et al. 2020). Thus, collective development and management of land and water resources are needed to address extreme watershed conditions in this region, viz. excessive runoff, enhanced soil erosion, inadequate crop yield, and poor infiltration (Bhattacharyya et al. 2015; Choudhari et al. 2018; Sofi et al. 2021). Hence, it is crucial for decision-makers to comprehend the properties of the watershed and the associated hydrological processes, which can be investigated adequately by morphometric analysis.

Morphometric analysis implies a quantitative assessment and evaluation of the earth's surface's size, shape, and features (Agarwal 1998; Strahler 1964). The relief, areal, and linear morphometric characteristics of a drainage basin provide significant criteria for interpreting numerical analyses of drainage networks (Meshram et al. 2019; Meshram and Sharma 2017; Patel and Srivastava 2013). Several parameters, including lithology structure, geomorphic setup, soil characteristics, land use and land cover (LULC), and slope, contribute to the acceleration of soil loss in various climatic regions (Bhat et al. 2022; Costache et al. 2020; Singh and Pandey 2021b). A broad interpretation of the hydrologic response, including surface runoff, groundwater potential, and infiltration capacity, can be derived from morphometric analysis (Bhat et al. 2022). In data-scarce ungauged watersheds with limited geomorphological, soil, hydrological, and geological information, morphometric analysis offers improved insight and accuracy for predicting basin characteristics like travel-time, intensity, and peak time of erosional processes (Meraj et al. 2015).

Using morphometric and statistical characteristics of basins, researchers have estimated flood peaks by incorporating the concept of GIUH, particularly for the ungauged basin. This approach posits that excess rainfall follows various probabilistic flow paths through the channel and overland regions before reaching the catchment outlet (Gupta et al. 1980; Rigon et al. 2016; Rodríguez-Iturbe et al. 1979). In the study by Kumar et al. (2007), the Nash and Clark IUH method was applied in the ungauged Ajay catchment, India, to simulate the direct runoff hydrograph for the ten rainfall-runoff events. They found that both the Nash IUH and the Clark IUH model options from the HEC-1 package effectively estimated the hydrographs. Cudennec et al. (2004) explored the geomorphological dimensions of the unit hydrograph concept and found that integrating geomorphological parameters contributed to a better understanding of both unit hydrograph and geomorphologic unit hydrograph theories. Bamufleh et al. (2020) utilized the self-similarity method to compute equivalent Horton-Strahler ratios in a semi-arid area for GIUH hydrograph modeling. Their findings indicated that the Nash model was superior to the Fréchet model in accuracy. In most cases, the GIUH proved a reliable method for estimating flood response, especially in regions with undulating topography (Sahoo and Jain 2018). It effectively predicts and mitigates extreme precipitation events' impact on the hilly watersheds' hydrological response (Dimri et al. 2016; Pandey and Mishra 2021; Singh and Pandey 2021a).

The hydrological response of the basin is further affected by anthropogenic activities like deforestation, mining, and built-up construction, as they alter the natural landscape and its associated processes. In this regard, prioritizing watersheds is crucial in managing watersheds in terms of development programs, project cost, and type. To prioritize sub-basin, morphometric factors and land use-land cover information of watersheds are useful in the absence of extensive hydrological data, especially in an ungauged basin. Utilizing satellite-derived terrain information, like a digital elevation model (DEM), enables the computation of morphometric characteristics for a given watershed. Unlike the contours on topographic maps, which are discrete, digital elevation models can be seamlessly incorporated into a geographic information system (GIS) (Das et al. 2018; Horton et al. 2011; Moore and Burch 1986). Moreover, it may aid in evaluating distinct drainage basins from diverse climatic and geological regimes (Meshram and Sharma 2017). In addition, the morphometric analysis may be useful in a multitude of scenarios, including natural resource management, flood frequency studies, landslide susceptibility mapping, groundwater potential estimation, erosion mitigation, and watershed prioritization (Aher et al. 2014; Farhan et al. 2016; Sujatha and Sridhar 2017; Tesema 2022b; Tiwari and Kushwaha 2021).

So far, numerous methodologies have been employed to prioritize the sub-basins for soil erosion and landslide prevention. Abdeta et al. (2020), Chandniha and Kansal (2017), and Tesema (2022b) used the compounding method; Dubey and Jha (2022), Pathare and Pathare (2021), Shekar and Mathew (2022) used principle component analysis (PCA); Duulatov et al. (2021), Gharibreza et al. (2021), Maury et al. (2019), Singh and Kansal (2023), and Srinivasan et al. (2021) used the Revised Universal Soil Loss Equation (RUSLE); Kumar and Sarkar (2022), Shelar et al. (2022), and Yalcin et al. (2011) used the analytical hierarchy process (AHP), and Joshi et al. (2021), Meshram et al. (2019), Rahaman et al. (2015, 2015), Sridhar and Ganapuram (2021), and Yalcin et al. (2011) used fuzzy-AHP aimed at sub-watersheds prioritization for erosion control.

The present study also strives to systematically prioritize watersheds susceptible to soil erosion by employing a multifaceted methodology. This approach amalgamates morphometric analysis with the compound average method (CM) and Principal Component Analysis (PCA), hydrological assessment utilizing the Geomorphological Instantaneous Unit Hydrograph (GIUH) technique, and semi-empirical modeling with the Revised Universal Soil Loss Equation (RUSLE). The GIUH method's rationale lies in its efficacy in identifying regions prone to flash flood impacts. At the same time, the morphometric approach, integrating CM and PCA, effectively identifies zones with maximum landslide potential. Moreover, the RUSLE model prioritizes the sub-watersheds based on annual soil erosion loss. In the past three decades, the region has experienced substantial soil erosion instigated by natural disasters such as cloudbursts, flash floods, and ensuing landslides (Kansal and Singh 2022; Singh and Kansal 2022a). This research distinguishes itself in flash flood-induced erosion studies through several novel contributions. Firstly, it adopts a comprehensive approach, amalgamating morphometric, hydrological, and semi-empirical methods—a holistic blend seldom observed in prior studies, offering a more nuanced understanding of landslide complexities. Such an integrated approach yields a more robust evaluation of sub-watershed vulnerability than standalone methods. This research further sets itself apart by emphasizing a targeted analysis at the sub-watershed level, promoting localized mitigation strategies, contrasting with many studies focusing on broader regions or basins. The Alaknanda River basin, with its unique geographic and climatic intricacies, stands as the focal point of this study, addressing its distinct vulnerabilities. Additionally, by incorporating field investigations pertaining to soil erosion events from the past three decades, the study presents an updated and contemporary perspective on challenges in the basin of the Indian Himalayan Region.

Material and methods

Datasets and tools

In this research, the main datasets employed consist of the digital elevation model (DEM) acquired from the Shuttle-Radar Topography Mission (SRTM), which can be accessed through the Open Topography portal (https://portal.opentopography.org/). The DEM hydro-processing and watershed delineation are performed using the "Hydrologic Engineering Center Geospatial Hydrologic Modeling Extension" (HEC-GeoHMS) extension (Hydrologic Engineering Center) of ArcGIS 10.5. The resulting small sub-watersheds are merged into 12 major sub-watersheds using the basin merge tool. Then, the morphometric analysis is performed using the ArcGIS Morphometric tool extension (Ayad Ali Faris Beg 2015). Rainfall data for individual sub-basins from 1990 to 2022 are extracted using the Climate Hazards Group InfraRed Precipitation with Station (CHIRPS) dataset available at the Climate Engine portal (http://climateengine.org). Furthermore, a connection is established between the sub-watershed prioritization and past landslides and flash-flood inventories in the region. These locations are essential for identifying the region's susceptibility, hazard, and risk of disasters. The landslide inventories for the Alaknanda River basin are downloaded from the Bhukosh website (https://bhukosh.gsi.gov.in/) of the Geological Survey of India (GSI). The GSI has carried out landslide inventories in different parts of India using various techniques, including remote sensing, field surveys, and geological and geophysical investigations. The landslide inventories by GSI in these areas provide valuable information on the types of landslides, their causes, and their distribution. Additionally, a comprehensive catalogue of prior flash flood incidents is assembled by collating information from published sources (Mishra et al. 2022; Singh and Pandey 2021a; Singh and Kansal 2022b), as well as from reports and newspaper articles available on the official website of the South Asia Network on Dams, Rivers, and People (SANDRP).

Methodology

The methodology is divided into four parts, as shown in Fig. 1. Starting from the watershed delineation, which estimates each sub-watershed boundary shapefile and drainage network, morphometrical analysis is carried out in each sub-watershed to estimate its linear, areal, and relief aspects. Followed by prioritizing the sub-watersheds using the PCA, CM, GIUH, and RUSLE. Finally, an overall prioritization of the sub-watershed is estimated based on the weighted average score, and the observations and validations are made based on the landslide's inventories, flash-flood incidents, and field observations.

Watershed Delineation

For both hydrologic and environmental studies, watershed delineation is a common practice. Watersheds can be automatically derived from DEM using geographic information systems (GIS) technology because DEMs provide a good representation of the terrain. Automated watershed delineation methods have existed since the 1980s when they were first implemented in GIS (Fairfield and Leymarie 1991). The watershed delineation using the terrain pre-processing function of HEC-GeoHMS extension of ArcGIS incorporates "Fill Sink, Flow Direction, Flow accumulation, Stream Definition and Segmentation, Catchment Grid and polygon formation, and Drainage Line processing."

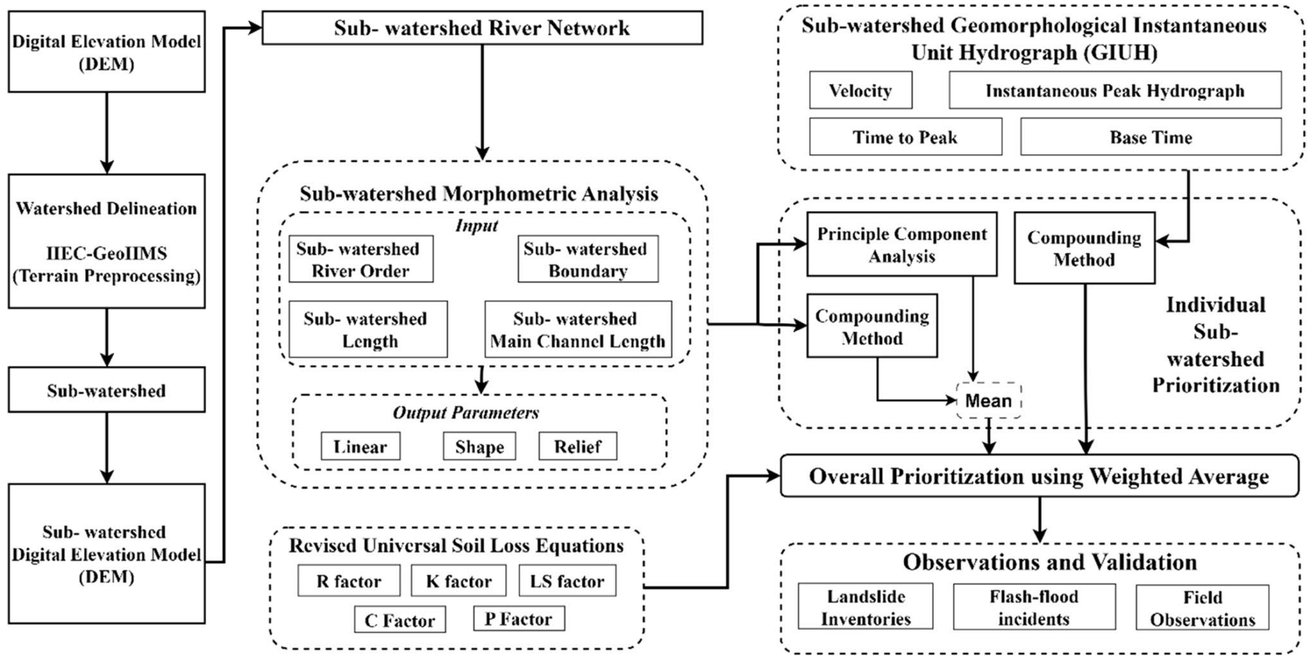

Fig. 1 Flowchart of the methodology

Sub-watershed morphometric analysis

The morphometric analysis uses the input parameters, viz., sub-watershed-wise river order, boundary area and length, and main-channel length. By calculating the geometry of the sub-basin polygons, their areas and perimeters were determined. Stream orders were determined from Strahler's method (Strahler 1952). From the analysis, about thirteen important parameters influencing landslides and soil erosion are taken, namely, "Mean Bifurcation Ratio (Rb), Drainage density (Dd), Stream frequency (Fs), Circularity ratio (Rc), Form factor (Rf), Elongation ratio (Re), Drainage Texture (T), Length of overland flow (Lo), Compactness Coefficient (Cc), Relief ratio (Rh), Relative relief (Rr), Ruggedness number (Rn) and average Slope (S)." The formula and the relationship used for the morphometric analysis are shown in Table 1.

Sub-watershed prioritization using Compounding average Method (CM)

In order to prioritize sub-watersheds, linear parameters are ranked based on their values, with the highest value assigned a rank of 1, the next highest a rank of 2, and so forth. The erodibility of a region is directly related to linear drainage parameters like T, Rb, Dd, Fs, and Lo (Nookaratnam et al. 2005). Shape parameters such as Re, Cc, Rc, and Rf vary inversely with erodibility (Meshram and Sharma 2017; Rai et al. 2009). The shape parameters are ranked based on their absolute values in ascending order. The parameter with the lowest value is given a rank of 1, the next lowest is given a rank of 2, and so on. The stream gradient, which is determined by the relief parameters, such as Rh, Rr, Rn, and S, directly impacts channel erosion, runoff, and the lag time of water during high-flow events (Panwar et al. 2017). Therefore, relief parameters were ranked in descending order, with the highest value receiving a rank of 1, the next highest receiving a rank of 2, and so on. Equal weights are assigned to all the morphometric parameters. Now, the rank of each sub-watershed is combined using the compounding average method. The CM approach adds the ranked values of all thirteen parameters across the chosen twelve sub-watersheds as composite parameters. Ultimately, the average values of these composite parameters are employed to establish the final priority. The highest priority is given to the lowest average value and vice versa (Bhattacharya et al. 2021; Chandniha and Kansal 2017; Pathare and Pathare 2021; Shekar and Mathew 2022; Tesema 2022a).

Sub-watershed prioritization using Principal Component Analysis (PCA)

PCA is a technique used for reducing the dimensionality of a large set of correlated variables to a smaller set of uncorrelated variables. This is achieved by transforming the original variables to a new set of orthogonal axes, which generates new principal components (PCs) that are uncorrelated with each other (Dubey 2022; Meshram and Sharma 2017; Shekar and

Table 1 Relationships used in Morphometric analysis

Parameters and aspects	Formula/method	Unit	Reference
Basin parameters			
Area (A)	GIS Analysis from DEM	km^2	-
Perimeter (P)	GIS Analysis from DEM	km	-
Maximum elevation (H)	Analysis from DEM	m	-
Minimum elevation (h)	Analysis from DEM	M	-
Length	$L_b = 1.312 \times A^{0.568}$	M	(Nookaratnam et al. 2005)
Stream order (U)		-	(Strahler 1964)
Stream number	$Nu = Nu_1 + Nu_2 + \cdots + N$	-	(Horton 1945);
Stream length	$Lu = Lu_1 + Lu_2 + \cdots + Lun$ average	km	(Horton 1945); (Strahler 1964)
Derived parameters			
Linear aspects			
Mean stream length (Lsm)	Average stream length of all orders	km	(Horton 1945)
Bifurcation ratio	$R_b = \frac{N_u}{N_{u+1}}$	-	(Schumm 1956)
Stream length ratio	$R_l = \frac{L_u}{L_{u+1}}$	-	(Horton 1945)
Mean bifurcation ratio	Average of bifurcation ratios of all orders	-	(Strahler 1964)
Mean stream length ratio	Average of stream length ratios of all orders	-	(Strahler 1964)
Stream frequency	$F_s = \frac{N_u}{A}$	km^{-2}	(Horton 1945)
Drainage density	$D_d = \frac{L_u}{A}$	km/km^2	(Horton 1945)
Drainage texture	$T = \frac{N_u}{P}$	km^{-1}	(Horton 1945)
Length of overland flow	$L_o = \frac{1}{(2D_d)}$	km	(Horton 1945)
Relief aspects			
Relief	$B_h = H - h$	km	(Strahler 1964)
Relief ratio	$R_h = \frac{B_h}{L_b}$	-	(Strahler 1964)
Relative relief	$R_{hp} = H \times \frac{100}{P}$	-	(Melton 1957)
Ruggedness number	$R_n = B_h \times D_d$	-	(Strahler 1964)
Areal/shape aspects			
Circulatory ratio	$R_c = 4\pi \frac{A}{P^2}$	-	(Miller 1953);
Elongation ratio	$R_e = \frac{2}{L_b} \times (\frac{A}{\pi})^{0.5}$	-	(Schumm 1956)
Form factor	$F_f = \frac{A}{L_b{}^2}$	-	(Horton 1945)
Compactness coefficient	$C_c = \frac{P}{2(\pi A)^{0.5}}$	-	(Horton 1945)

Mathew 2022). Maximum data variation is found in the first principal component (PC1), and variation gradually decreases in subsequent components. The new components are key in explaining the greatest possible variation in the original variables (Bhat et al. 2022). The original factor loading matrix and the rotational factor loading matrix are employed for the estimation. Summation and normalization of significant loadings from the four PCs yield the weights for each component. Finally, the sub-watersheds are ranked using the weighted sum method.

Sub-watershed prioritization using Geomorphological Instantaneous Unit Hydrograph (GIUH)

The GIUH is a hydrological model introduced by Rodríguez-Iturbe et al. (1979), which aimed to represent the relationship between rainfall and runoff in watersheds. The GIUH model considers that the hydrological response of a catchment is a result of the interactions between the rainfall and the physical characteristics of the catchment, such as its topography, soil, and vegetation cover. (Gupta et al.

(1980) and Rigon et al. (2016) further enhanced the GIUH model by incorporating the concept of travel time distribution. This enhancement involves dividing the catchment into sub-catchments, considering each has a different travel time distribution function.

The instantaneous hydrograph peak of the GIUH is given by,

$$q_p = (\frac{1.31}{L_\Omega})R_L^{0.43}v \tag{1}$$

The time to peak (t_p) of the GIUH is given by,

$$t_p = 0.44(\frac{R_B}{R_A})^{0.55} R_L^{-0.38}\frac{L_\Omega}{v} \tag{2}$$

$$t_b = \frac{2}{q_p} \tag{3}$$

where t_b = base time (hour), t_p = time to peak (hour); q_p = instantaneous hydrograph peak (/hour); v = dynamic parameter velocity (m/s), Ln = length of the highest order stream (km), and are R_A = stream-area ratio, R_B = bifurcation ratio, R_L = stream-length ratio.

To estimate the dynamic parameter velocity (V) for a watershed, a combination of velocity and the Kirpich formula can be employed, as suggested by Nongthombam et al. (2011)

$$t_c = 0.01947L^{0.77}S^{-0.385} \tag{4}$$

$$t_c = \frac{1}{60} \times \frac{L}{v} \tag{5}$$

$$v = 0.8562L^{0.23}S_B^{0.385} \tag{6}$$

where t_c = time of concentration (min), S_B = mean slope of the basin (m/m), and L = mainstream length (m).

Derivation of GIUH based on the Nash model The Nash Geomorphic Instantaneous Unit Hydrograph (GIUH), a distributed rainfall-runoff model, employs routing instantaneous inflow through linear reservoirs with equal storage coefficients. In a given watershed with "n" reservoirs, a unit pulse of rainfall is input over an infinitesimally short time $\Delta t \to 0$, generating an outflow with ordinate $u(t)$ representing the Instantaneous Unit Hydrograph (IUH).

Outflow resulting from the first reservoir is calculated using Eq. 7,

$$u_1(t) = -\frac{e^{-\frac{t}{k}}}{k} \tag{7}$$

The outflow $u_1(t)$ from the first reservoir flows into the second reservoir, given by,

$$u_2(t) = -\frac{e^{-\frac{t}{k}}}{k}(1 - e^{-\frac{t}{k}}) \tag{8}$$

Thus, continuing the same process for "n" no. of reservoirs, the resultant outflow, known as Nash model ordinate of IUH, is given by,

$$u(t) = (\frac{t}{k})^{a-1} \frac{e^{-\frac{t}{k}}}{k\Gamma(a)} \tag{9}$$

The Horton ratios and parameters of the gamma distribution are mathematically related, where $u(t)$ represents the ordinate of IUH (hour^{-1}), t represents time interval sampling (hour), Γ (a) is the gamma function, and n and k are parameters of the Nash model, representing number of linear reservoirs and storage coefficient (hour), respectively.

Estimation of geomorphological parameter of Nash model Connecting the scale (k) and shape parameter (n) of the Nash model with the q_p and t_p of GIUH, one can fully determine the shape of GIUH. On substituting and simplifying Eq. 9 (Rai et al. 2009),

$$\frac{\partial \ln[u(t)]}{\partial t} = [-\frac{1}{k} + \frac{(n-1)}{t}] \tag{10}$$

$$\frac{(n-1)}{\Gamma(n)}\exp[-(n-1)](n-1)^{n-1} = 0.5764(\frac{R_B}{R_A})^{0.55} R_L^{0.05} \tag{11}$$

The "n" parameter is determined by solving Eq. 11 through the Newton–Raphson method, while the estimation of the "k" value for a specific "v" value is done using Eq. 12, given by,

$$k = 0.44(\frac{R_B}{R_A})^{0.55} R_L^{0.05} \frac{1}{(n-1)} \frac{L_\Omega}{v} \tag{12}$$

The estimated instantaneous hydrograph peak, velocity, and time to the peak are then used to identify the critical sub-watershed vulnerable to flash-flood impacts. The sub-watershed with a high value of velocity, instantaneous hydrograph peak, and low value of time to peak is given high priority. This information helps develop flood warning systems and mitigate future flash flooding risks. Identifying critical sub-watersheds is crucial in minimizing the impact of flash floods.

Sub-watershed prioritization using Revised Universal Soil Loss Equations (RUSLE) (obtained from Singh and Kansal 2023)

RUSLE is a model that employs a comprehensive series of mathematical equations to estimate the average annual soil loss and sediment yield due to inter-rill and rill erosion processes (Renard et al. 1997) and is denoted as per Eq. 13:

$$\mathbf{A} = \mathbf{R} \times \mathbf{K} \times \mathbf{LS} \times \mathbf{C} \times \mathbf{P} \tag{13}$$

In the given equation, the rainfall-runoff erosivity factor is represented by R (MJ mm ha^{-1} h^{-1} year^{-1}), which considers various rainfall characteristics, including volume, duration, and intensity. The average annual soil loss is given by A (ton ha^{-1} year^{-1}). In this study, the annual average precipitation (AAP) data from 1991 to 2020 is extracted at grid locations and interpolated for the basin to estimate the rainfall erosivity factor using Eq. 14 by (Das et al. 2018; Dutta et al. 2015; Sandeep et al. 2021; Singh et al. 1981):

$$\mathbf{R} = 79 + 0.363 \times \mathbf{AAP} \tag{14}$$

The soil erodibility factor K (t ha h ha^{-1} MJ^{-1} mm^{-1}) represents the resistance of soil particles to erosion caused by storm events. It is typically determined by examining a specific location's soil and surface characteristics (Wischmeier and Smith 1978). To estimate soil characteristics, the NBSS-LUP soil map is vectorized using ArcGIS software. K values are calculated through nomographs that consider soil structure, soil texture and permeability, and percentage of silt, clay, organic matter, and sand (Wischmeier and Smith 1978). Equations 15 and 16 are utilized to determine the K factor.

$$\mathbf{K} = \frac{2.1 \times 10^{-4}(12 - \mathbf{OM})\mathbf{M}^{1.14} + 3.25(\mathbf{s} - 2) + 2.5(\mathbf{p} - 3)}{759.4} \tag{15}$$

The variables used in this context are as follows: s represents soil structure code, p represents soil permeability code, OM represents %organic matter, and M denotes the primary soil particle size fraction, given by:

$$\mathbf{M} = (\%\mathbf{silt} + \%\mathbf{sand}) \times (100 - \%\mathbf{clay}) \tag{16}$$

The topographic steepness factor, or LS, represents the combined effect of slope length and steepness on soil loss rates (Batar and Watanabe 2021; Biswas et al. 2021; Das et al. 2020). So, in this study, the LS factor values are estimated using the Eq. 17 given by (Moore and Burch 1986) as:

$$LS = 1.4 \times (Flow\ accumulation \times \frac{Cell\ Size}{22.13})^{0.4} \times (\frac{sin\ slope}{0.0896})^{1.3} \tag{17}$$

In this equation, cell size denotes the grid cell size or DEM resolution, and sin slope refers to the slope degree value.

For determining the C factor, this study employs the method introduced by Van der Knijff et al. (2000) as they found that the C factor does not exhibit a linear relationship with NDVI (Normalized Difference Vegetation Index) but rather decreases exponentially, given as per Eq. 18:

$$\mathbf{C} = \mathbf{exp}[-\alpha \frac{\mathbf{NDVI}}{\beta - \mathbf{NDVI}}] \tag{18}$$

In this case, α and β are parameters defining the NDVI-C curve shape, with $\alpha = 2$ and $\beta = 1$. The C factor, also known as the cover and cropping management factor, describes the influence of vegetation cover on soil erosion rates, as vegetation prevents rainwater from directly contacting soil particles and causing erosion (Das et al. 2020).

The supporting practices factor, represented by P, signifies the ratio of soil erosion caused by a specific support practice to the soil loss produced by straight-line tillage in both uphill and downhill directions, which yield equivalent soil loss amounts (Ganasri and Ramesh 2016). The estimation of the P factor value, which varies from 0 to 1 (as shown in Table 2), considers the basin's land use and land cover (LULC). A "P" factor value of 1 indicates that no effective conservation practices have been implemented. The RUSLE model integrated with GIS technology can comprehensively estimate soil erosion by predicting soil loss at a pixel level. Additionally, it is worth noting that the P, C, and LS values used in this model are dimensionless (Das et al. 2018; Dutta et al. 2015).

This study is crucial for understanding and addressing the flash flood-induced erosion contributing to significant soil loss and degradation of pedosphere strata in the Indian Himalayan Region. Thus, the Alaknanda River basin is chosen as a case study for the analysis due to the confluence of factors exacerbating this phenomenon, including extreme precipitation events, undulating topographical features, and suboptimal soil and water conservation methodologies.

Study area

The Alaknanda basin in Uttarakhand, India, is part of the upper Ganga basin and has an outflow at Rudraprayag (Fig. 2). It has a basin size of 10272 sq km. The Bhagirath Kharak and Satopanth Glaciers, situated within the western Garhwal Himalayas, form the Alaknanda River Basin. This basin lies in Uttarakhand, with geographic coordinates spanning 78°45′ E to 80°15′ E in

Table 2 Commonly used conservation practice (P) factors as per the LULC

S. No	Class	P factor*
1	Cropland	0.45
2	Built-up	0.1
3	Forest	1
4	Shrubland	1
5	Barren land	1
6	Fallow land	0.6
7	Water bodies/glacier/snow	-

*Sources: data compiled by the author based on statistics provided in the literature

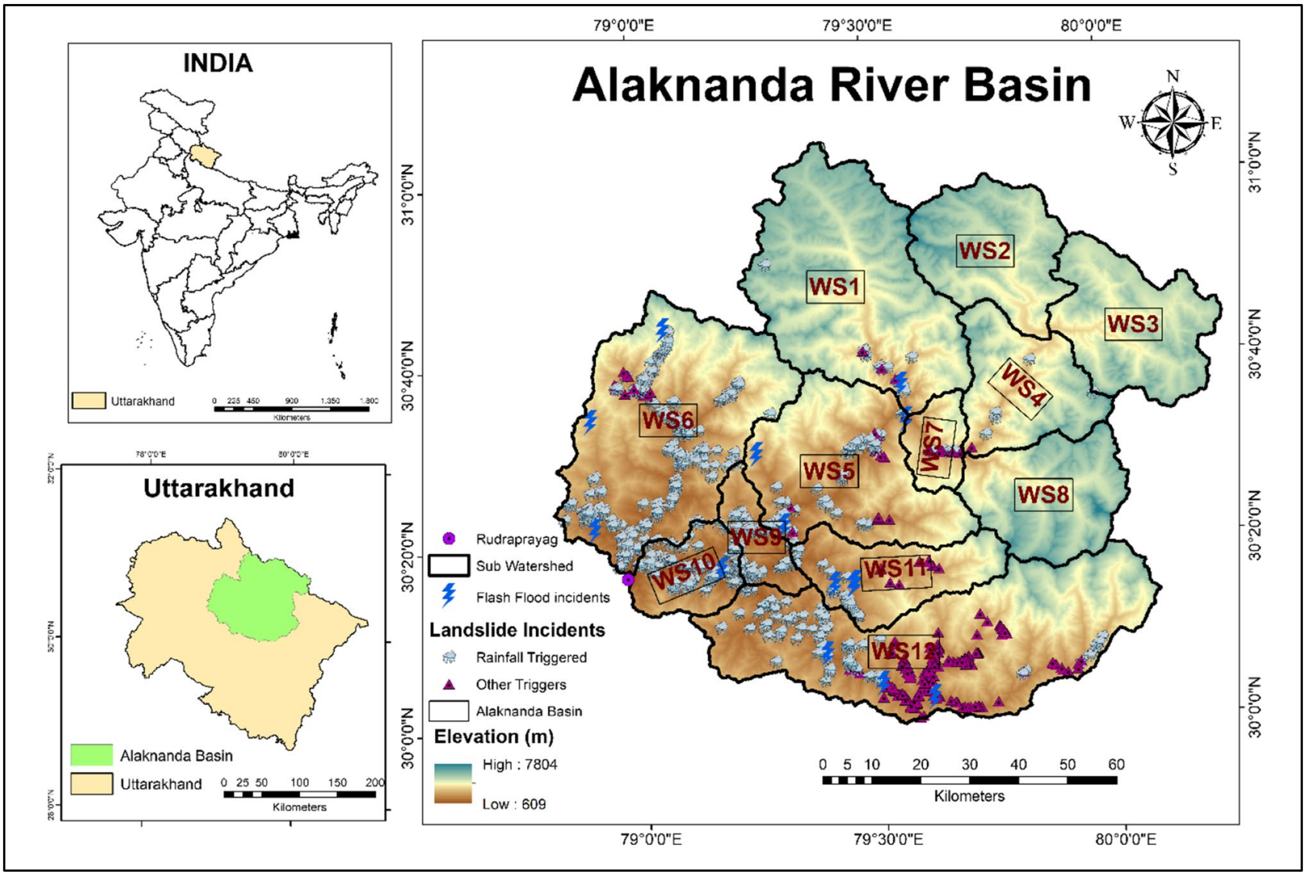

Fig. 2 Alaknanda River basin showing landslide occurrence and flash-flood sites

longitude and 30°10′ N to 31°5′ N in latitude. Elevations within the region vary between 609 and 7804 m above sea level. The study area's northern section experiences a severe winter climate. The region is dominated by a tropical monsoon climate, with roughly 75% of annual precipitation, averaging 1600 mm, between June and September (Panwar et al. 2016; Singh and Kansal 2020). The area's vulnerability to natural disasters, such as earthquakes, landslides, flash floods, and cloudbursts, makes it susceptible to soil erosion and landslides.

Over the past three decades, the Alaknanda River basin in Uttarakhand has experienced numerous severe weather incidents, leading to flash floods, landslides, and erosions. The river basin's districts of Chamoli and Rudraprayag have been particularly affected by such events, including flash floods, landslides, and cloudbursts. As a result, mudslides, stream erosion, and debris movement downstream have caused extensive damage to properties, bridges, and other human-made infrastructure (Azmeri et al. 2016; Singh and Pandey 2021b). In February 2021, an avalanche-induced flash flood occurred in the Chamoli district's Rishiganga and Dhauliganga river watersheds. This disaster claimed the lives of approximately 200 people and inflicted severe damage on the Rishiganga and Tapovan Vishnugad hydropower projects. Furthermore, the catastrophe led to riverbank collapse, scouring, erosion, bridge congestion, debris flows, and sediment deposition. (Mishra et al. 2022; Singh et al. 2023; Singh and Kansal 2022a). In October 2022, a landslide hit three houses in the Tharali area of Uttarakhand's Chamoli district due to landslides. Four people were killed and another injured in the incident. In May 2023, a landslide blocked the Badrinath highway in Uttarakhand's Chamoli, leaving several tourists stranded. Escalating human activities, including hydropower projects, tourism, and construction, have placed tremendous stress on the region's delicate ecosystem, resulting in a rise in natural disasters. Despite expert warnings, these activities persist in endangering the region's ecological equilibrium and the livelihoods of those who rely on it.

Results

Morphometric parameters estimation

Linear parameters

The linear parameter of morphometry is a set of measurements used to describe a watershed's size, shape, and drainage characteristics. Stream order, stream network length, watershed perimeter, and longest flow path are important linear parameters. Other morphometric parameters commonly include area, slope, elevation, and shape measurements. These parameters are useful for understanding and managing regional water and land use interactions.

Stream number (Nu): The number and size of streams in a region are largely influenced by their physiography, geomorphology, and geology (Rai et al. 2017). Nu is important in understanding the structure and function of river systems, as different orders of streams have distinct characteristics in terms of flow, sediment transport, and ecological processes. In this study, WS12 has the highest Nu, with 525 first-order, 112 s-order, 25 third-order, 5 fourth-order, and 1 fifth-order streams, as shown in Table 3 and Fig. 3.

Stream length (Lu): Lu is an important parameter in hydrology, as it can be used to estimate the volume and velocity of water flow within a watershed and predict the potential for flooding or erosion. It measures the total length of a river or stream channel within a given watershed or drainage basin. In all sub-watersheds, the Lu is the longest for the first order, decreasing with an increase in the stream order (Table 3). The basin has a total stream length of 6825.1 km, with 3546.8 km for first-order streams, 1578.7 km for second-order streams, 838.5 km for third-order streams, 551.2 km for fourth-order streams, 300.6 km for fifth-order streams, and 9.2 km for sixth-order streams. The WS12 has a maximum Lu of 1206.2 km, while the WS7 has a minimum Lu of 136.2 km.

Bifurcation ratio (Rb): Rb is an important parameter in understanding the structure and function of river systems, as it can provide insight into the connectivity and branching patterns of streams within a network. High bifurcation ratios indicate a more branching, dendritic pattern, while low ratios indicate a more linear, trellis-like pattern (Horton 1945; Rathore et al. 2022; Sridhar and Ganapuram 2021). Rb indicates relief and erosion. The Rb ranges between 3.6 (WS6) and 5.72 (WS11), as shown in Table 3.

Drainage density (Dd): Dd is a geomorphological parameter that describes the degree of stream branching and the efficiency of water flow through a watershed. It is defined as the total length of all stream channels in a drainage basin per unit area of the basin. The Dd of a watershed is influenced by several factors, including climate, topography, geology, and vegetation cover (Farhan et al. 2016). Regions with highly permeable materials

Table 3 Sub-watershed wise stream order and numbers

Sub-watershed no	Parameter	Stream order					
		I	II	III	IV	V	VI
WS1	No. of streams	445	108	25	6	1	
	Stream length (km)	571.3	226.1	166.4	67.9	46.7	
WS2	No. of streams	215	45	9	2	1	
	Stream length (km)	276.2	128.1	61.7	40.4	25.2	
WS3	No. of streams	221	50	12	3	1	
	Stream length (km)	275.3	102.8	63.4	40.1	17.4	
WS4	No. of streams	179	36	9	2	1	
	Stream length (km)	206.8	97.2	43.3	30.6	22.1	
WS5	No. of streams	292	61	13	4	1	
	Stream length (km)	339.1	163.9	70.2	64.0	26.0	
WS6	No. of streams	453	91	19	7	2	1
	Stream length (km)	519.2	249.8	139.1	87.9	37.5	9.2
WS7	No. of streams	53	11	3	1		
	Stream length (km)	80.6	35.7	11.3	8.5		
WS8	No. of streams	209	52	14	4	1	
	Stream length (km)	293.6	129.5	46.0	39.5	25.2	
WS9	No. of streams	62	14	2	1		
	Stream length (km)	70.2	39.8	29.3	7.5		
WS10	No. of streams	90	17	6	1		
	Stream length (km)	121.9	47.7	35.0	30.1		
WS11	No. of streams	150	35	9	1		
	Stream length (km)	186.6	80.0	31.0	54.6		
WS12	No. of streams	525	112	25	5		
	Stream length (km)	605.8	278.2	141.7	80.0		

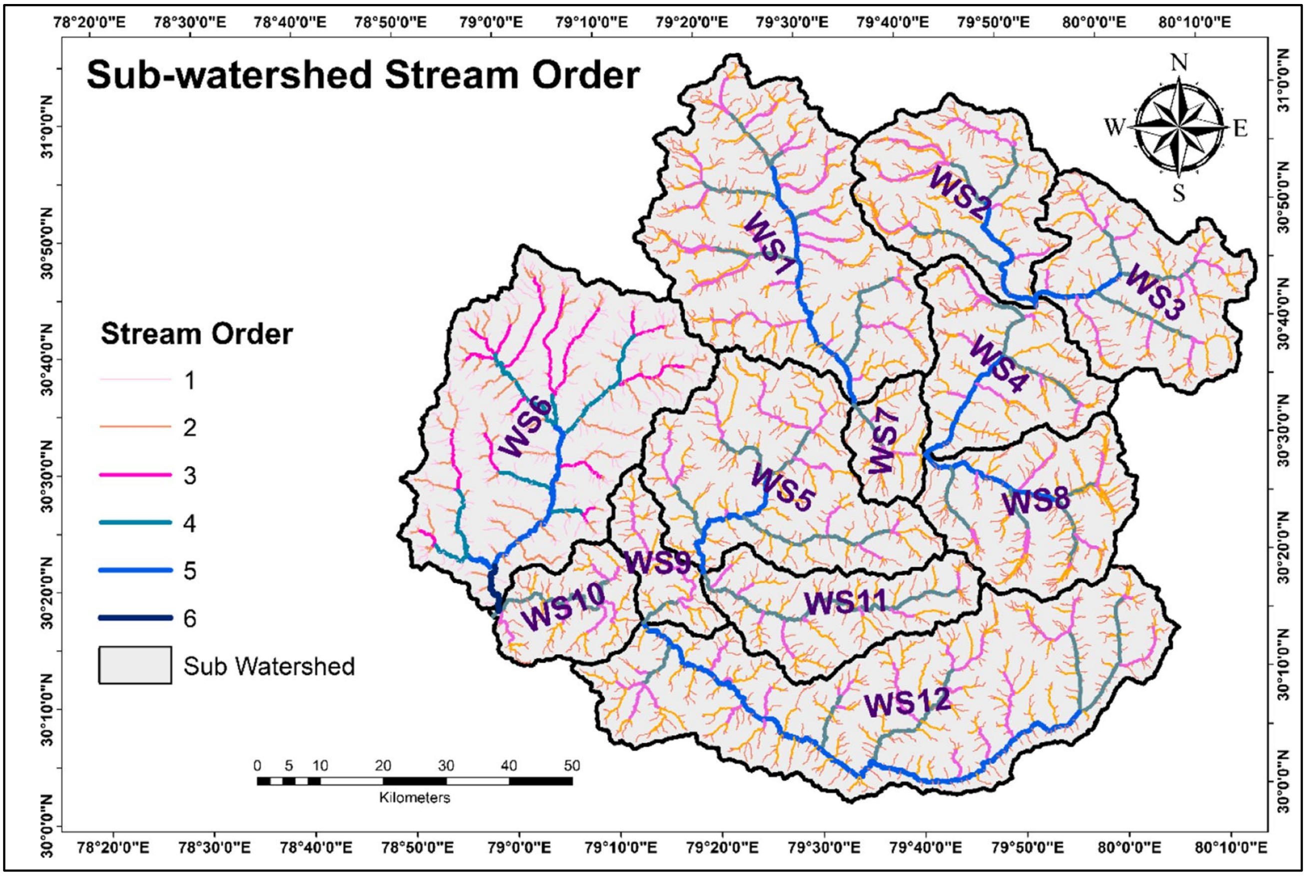

Fig. 3 Stream order in various sub-watersheds of Alaknanada Basin

and vegetation cover, as well as low relief, tend to exhibit a low drainage density (Dd) value, while Dd values tend to be high in regions with impermeable subsurface material, mountainous relief, and sparse vegetation (Gayen et al. 2019; Halder et al. 2021; Rathore et al. 2022). In the study area, Dd ranges between 0.62 (WS5) and 0.78 (WS8), as shown in Table 4.

Stream frequency (Fs): Fs measures the number of stream channels that intersect a given area within a drainage basin (Horton 1932). A high stream frequency value indicates a larger surface runoff, resulting in an early peak discharge. In contrast, a low stream frequency value indicates a landscape with high permeability and low relief. It has been noticed that high Fs are observed in WS8 (0.38) and low Fs in WS7 (0.33), as shown in Table 4.

Drainage Texture (T): T refers to the degree of channel spacing in a topography that rivers have dissected, and various factors such as vegetation, climate, precipitation, infiltration ability, soil characteristics, rock type, and extent of landscape development influence T values (Smith 1950). WS1 has a maximum $T=2.13$, while WS9 has a minimum $T=0.9$ (Table 4).

Length of overland flow (Lo): Lo is a parameter describing the distance water travels as overland flow before it reaches a stream channel. The Lo ranges between 0.31 (WS5) and 0.39 (WS8), as shown in Table 4.

Areal parameters

The areal parameters of morphometry are used to characterize the physical properties of a watershed and help to understand the hydrological processes that occur within it.

Compactness coefficient (Cc): Cc measures the shape complexity of a basin. A higher value of Cc indicates a more compact and spherical shape, while a lower value indicates a more irregular and elongated shape (Horton 1945). The WS has the maximum Cc=2.33, while WS10 has the minimum $T=1.71$ (Table 4).

Circularity ratio (Rc): The Rc is used to describe the shape of a basin (Miller 1953). Basins with higher circularity ratios tend to have more uniform drainage patterns. They may be more resilient to changes in water flow and sediment transport, while basins with lower circularity ratios may be more susceptible to erosion and sedimentation in certain areas. Rc ranges between 0.19 (WS12) and 0.35 (WS10), as shown in Table 4.

Table 4 Morphometric analysis results of Alaknanda sub-watersheds

Sub-watershed	Mean bifurcation ratio (Rb)	Drainage density (Dd)	Stream frequency (Fs)	Drainage texture (*T*)	Length of overland flow (Lo)	Compactness Coefficient	Circularity ratio (Rc)	Form factor (Rf)	Elongation ratio (Re)	Relief ratio (Rh)	Relative relief (Rr)	Ruggedness number (Rn)	Average slope (*S*)
		km/ sq km			km								
WS1	4.65	0.70	0.38	2.13	0.35	1.99	0.26	0.44	0.75	0.11	2.29	4.42	0.66
WS2	4.07	0.74	0.38	1.57	0.37	1.83	0.30	0.51	0.80	0.13	2.77	3.53	0.62
WS3	3.9	0.64	0.37	1.46	0.32	2.01	0.25	0.62	0.89	0.12	2.10	2.67	0.62
WS4	3.87	0.65	0.37	1.39	0.32	1.87	0.29	0.59	0.87	0.16	3.15	3.32	0.77
WS5	4.18	0.62	0.35	1.60	0.31	2.02	0.25	0.70	0.94	0.14	2.32	3.34	0.68
WS6	3.6	0.64	0.35	2.09	0.32	1.92	0.27	0.49	0.79	0.11	2.32	4.05	0.61
WS7	3.83	0.66	0.33	0.77	0.33	1.74	0.34	0.64	0.90	0.24	4.90	2.84	0.68
WS8	3.81	0.78	0.41	1.74	0.39	1.74	0.33	0.57	0.86	0.17	3.66	4.58	0.68
WS9	4.48	0.66	0.36	0.70	0.33	2.15	0.22	0.35	0.67	0.12	2.57	1.92	0.57
WS10	4.71	0.70	0.34	1.03	0.35	1.71	0.35	0.58	0.86	0.10	2.17	1.67	0.60
WS11	5.72	0.65	0.36	1.14	0.32	2.08	0.23	0.27	0.59	0.14	3.66	4.05	0.63
WS12	4.79	0.64	0.35	1.88	0.32	2.33	0.19	0.26	0.58	0.07	1.70	3.87	0.63

Form factor (Rf): The Rf is often used to evaluate the shape of watersheds, which can affect the distribution of water and sediment within the basin. The smaller value indicates a more elongated basin. The Rf ranges between 0.26 (WS12) and 0.70 (WS5), as shown in Table 4.

Elongation ratio (Re): Re is a geomorphometric parameter that describes the shape of a watershed and helps understand its hydrological nature. Re ranges between 0.58 (WS12) and 0.94 (WS5), as shown in Table 4.

Relief parameters

Relief parameters in morphometry refer to the measurement of variations in elevation or vertical differences across the surface of a landscape. These parameters are essential in understanding a watershed's topography and its role in controlling the movement of water and other substances through the landscape. Understanding the relief parameters of a landscape is crucial in determining the spatial distribution of water and sediment and identifying areas of potential erosion or flooding.

Relief ratio (Rh): Rh is a morphometric parameter used to measure the overall steepness of the terrain within a defined area. High relief ratios indicate steeper slopes and more rugged terrain, which can increase the likelihood of erosion and landslides during heavy precipitation events. Basins with steeper slopes typically exhibit faster runoff, resulting in more pronounced peak discharges and increased erosive potential (Bhattacharya et al. 2021; Chandniha and Kansal 2017). The Rh ranges between 0.07 (WS12) and 0.24 (WS7), as shown in Table 4.

Relative relief (Rr): The elevation difference between the maximum and minimum points in a landscape relative to its perimeter is described by Rr. Watersheds with high Rr values tend to have steep slopes and rugged terrain and are more susceptible to erosion and sediment transport. The Rr value ranges between 1.70 and 4.90, as shown in Table 4.

Ruggedness number (Rn): Rn measures the topographic variability of the landscape and provides a quantitative measure of the ruggedness or roughness of the terrain. The Rn value ranges between 1.67 (WS10) and 4.58 (WS8), as shown in Table 4.

Average slope (*S*): *S* is a measure of the steepness of the land surface within the watershed and thus influences the flow of water and affects erosion and sediment transport. A high average slope generally indicates a steep and rugged terrain, while a low average slope indicates a flatter landscape. The *S* value varies from 0.57(WS9) to 0.77(WS4), as shown in Table 4.

Morphometry-based compounding average method (CM)

Using the compounding method, Table 5 displays the final scores and rankings for all twelve sub-watersheds. The highest and lowest prioritized scores among the sub-watersheds are 8.2 (WS3) and 4.1 (WS8), respectively (Fig. 4). A higher score indicates a higher degree of erosion in a particular sub-watershed and, therefore, a higher priority for conservation or restoration efforts.

Table 5 The sub-watershed prioritization map using the compounding approach

Sub-watershed	Rb	Dd	Fs	*T*	Lo	Cc	Rc	Rf	Re	Rh	Rr	Rn	S	Compound average	Priority
WS1	4	3	2	1	3	7	6	4	4	10	9	2	5	4.6	2
WS2	7	2	3	6	2	4	9	6	6	6	5	6	9	5.5	4
WS3	8	9	4	7	9	8	5	10	10	7	11	10	8	8.2	12
WS4	9	8	5	8	8	5	8	9	9	3	4	8	1	6.5	6
WS5	6	12	10	5	12	9	4	12	12	5	7	7	3	8.0	10
WS6	12	11	9	2	11	6	7	5	5	9	8	4	10	7.6	9
WS7	10	6	12	11	6	2	11	11	11	1	1	9	4	7.3	8
WS8	11	1	1	4	1	3	10	7	7	2	3	1	2	4.1	1
WS9	5	5	7	12	5	11	2	3	3	8	6	11	12	6.9	7
WS10	3	4	11	10	4	1	12	8	8	11	10	12	11	8.1	11
WS11	1	7	6	9	7	10	3	2	2	4	2	3	6	4.8	3
WS12	2	10	8	3	10	12	1	1	1	12	12	5	7	6.5	5

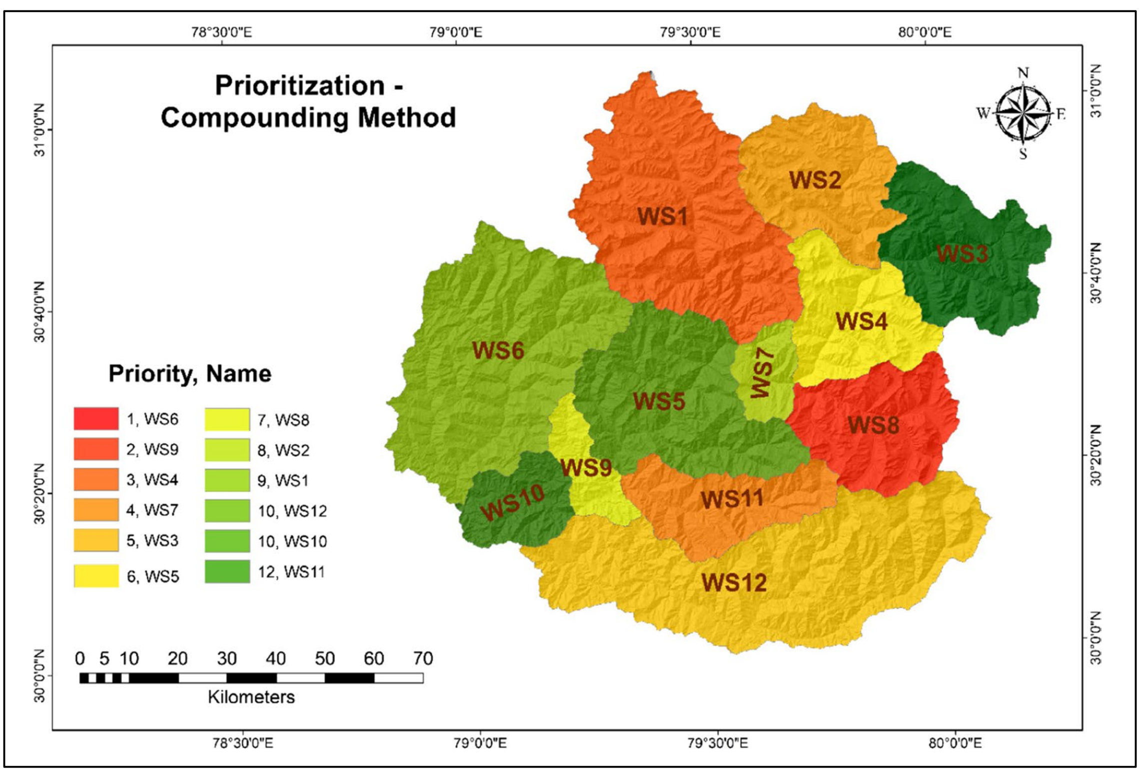

Fig. 4 The sub-watershed prioritization map using the compounding approach

Morphometry based-PCA approach

Intercorrelation among the morphometric parameters

The PCA is exclusively utilized for morphometric analysis to decrease the number of dimensions (Madiona et al. 2019). Utilizing SPSS 25.0 software, the inter-correlation analysis of the morphometric parameters is conducted for the Alaknanda sub-watershed. The correlation matrix, consisting of 13 geomorphic parameters, revealed strong associations between Dd and Lo, Rc and Cc, Rf and Re, and Rh and Rr. Furthermore, high correlations, with correlation coefficients ranging from 0.7 to 0.9, are observed between Rb and Rf, between Rb and Re, between Re and Cc, and between *T* and ruggedness number (Rn). Some moderate correlations (correlation coefficient between 0.5 and 0.7) exist between Dd and Fs, between Dd and Rc, Dd and Cc, Fs and Lo, Fs and Rn, Rc and Rf, Rc and Re, Rc and Lo, Rc and Rh, Rc and Rr, Rf and Cc, Rf and Rh, Re and Rh, Lo and Cc, Cc and Rh, Cc and Rr, and Rh and S. At this stage, it is challenging to group the parameters into components, so to simplify the process, the next step involves applying principal component analysis to the correlation matrix (Table 6).

First-factor loading matrix The correlation matrix of 13 geomorphic parameters generates the first factor loading matrix. As shown in Table 7, the first four components account for approximately 89.71% of the total variance in the Alaknanda watershed. Table 8 indicates that the first component exhibits a very high correlation with Cc and Rc, a high correlation

Table 6 Intercorrelation matrix of the morphometric parameters

	Rb	Dd	Fs	Rc	Rf	Re	T	Lo	Cc	Rh	Rr	Rn	S
Rb	1.00	−0.13	−0.15	−0.44	−0.70	−0.72	−0.19	−0.16	0.47	−0.37	−0.11	0.01	−0.31
Dd	−0.13	1.00	0.69	0.57	0.08	0.12	0.12	1.00	−0.56	0.14	0.23	0.25	−0.01
Fs	−0.15	0.69	1.00	0.05	−0.02	0.02	0.42	0.67	−0.12	−0.03	−0.01	0.53	0.21
Rc	−0.44	0.57	0.05	1.00	0.66	0.69	−0.22	0.57	−0.98	0.56	0.50	−0.17	0.27
Rf	−0.70	0.08	−0.02	0.66	1.00	1.00	−0.06	0.09	−0.69	0.50	0.20	−0.23	0.44
Re	−0.72	0.12	0.02	0.69	1.00	1.00	−0.05	0.14	−0.72	0.50	0.20	−0.23	0.43
T	−0.19	0.12	0.42	−0.22	−0.06	−0.05	1.00	0.13	0.17	−0.45	−0.48	0.76	0.15
Lo	−0.16	1.00	0.67	0.57	0.09	0.14	0.13	1.00	−0.55	0.12	0.20	0.23	−0.04
Cc	0.47	−0.56	−0.12	−0.98	−0.69	−0.72	0.17	−0.55	1.00	−0.58	−0.51	0.11	−0.29
Rh	−0.37	0.14	−0.03	0.56	0.50	0.50	−0.45	0.12	−0.58	1.00	0.93	0.01	0.52
Rr	−0.11	0.23	−0.01	0.50	0.20	0.20	−0.48	0.20	−0.51	0.93	1.00	0.11	0.40
Rn	0.01	0	0.53	−0.17	−0.23	−0.23	0.76	0.23	0.11	0.01	0.11	1.00	0.35
S	−0.31	−0.01	0.21	0.27	0.44	0.43	0.15	−0.04	−0.29	0.52	0.40	0.35	1.00

Table 7 Total variance based on PCA

Component	Initial eigenvalues			Extraction sums of squared loadings			Rotation sums of squared loadings
	Total	% of variance	Cumulative %	Total	% of variance	Cumulative %	Total
1	5.15	39.62	39.62	5.15	39.62	39.62	4.16
2	2.95	22.71	62.33	2.95	22.71	62.33	3.29
3	1.92	14.79	77.12	1.92	14.79	77.12	2.32
4	1.64	12.60	89.71	1.64	12.60	89.71	3.29
5	0.54	4.16	93.87				
6	0.48	3.66	97.53				
7	0.22	1.65	99.19				
8	0.10	0.73	99.92				
9	0.01	0.05	99.97				
10	0.00	0.03	100.00				
11	0.00	0.00	100.00				
12	0.00	0.00	100.00				
13	0.00	0.00	100.00				

Table 8 Unrotated matrix

Parameters	Component			
	1	2	3	4
Cc	−0.924	−0.011	0.151	0.165
Rc	0.907	−0.02	−0.208	−0.185
Re	0.816	−0.254	0.402	−0.262
Rf	0.796	−0.294	0.41	−0.242
Rh	0.747	−0.296	−0.142	0.534
Rb	−0.631	0.036	−0.511	0.21
Fs	0.227	0.838	0.04	0.05
Rn	−0.036	0.718	0.33	0.539
Dd	0.518	0.716	−0.418	−0.177
Lo	0.515	0.708	−0.404	−0.223
Dt	−0.162	0.672	0.657	−0.041
Rr	0.604	−0.171	−0.39	0.65
S	0.489	0.01	0.462	0.566

Table 9 Rotated matrix

Parameters	Components			
	PC1	PC2	PC3	PC4
Re	0.964	0.054	0.156	−0.065
Rf	0.956	0.008	0.168	−0.075
Rb	−0.82	−0.053	−0.015	−0.172
Cc	−0.656	−0.536	−0.388	0.187
Rc	0.627	0.542	0.388	−0.25
Dd	0.063	0.982	0.082	0.112
Lo	0.086	0.981	0.043	0.095
Fs	−0.013	0.644	−0.06	0.583
Rr	0.048	0.167	0.967	−0.066
Rh	0.353	0.05	0.906	−0.053
S	0.408	−0.166	0.542	0.534
Rn	−0.197	0.164	0.124	0.914
Dt	0.098	0.072	−0.474	0.819
Sum	1.917	2.909	2.439	2.563
Weights	0.20	0.30	0.25	0.26

with Re, Rf, and Rh, and a moderate correlation with Rb, Dd, Rr, and Lo. The second component is highly correlated with Fs, Rn, Dd, and Lo and moderately correlated with Dt. The third component is moderately correlated with Rb and Dt, while the fourth is moderately correlated with Rh, Rn, and S in the Alaknanda watershed. According to the analysis, certain parameters exhibit strong correlations, while others show moderate correlations with some components, and some parameters do not correlate with any. However, it is currently impossible to determine which components are significantly correlated. Thus, it is essential to rotate the initial factor loading matrix to enhance the correlation.

Rotation of the first-factor loading matrix The transformation matrix is multiplied with the selected components to create a rotated factor loading matrix (Table 9) from the first-factor loading matrix. It is observed that the first component is highly correlated with Re and Rf, highly correlated with Rb, and moderately correlated with Cc and Rc, all as determined by the rotated factor loading matrix. The second factor has a moderate correlation with Cc, Rc, and Fs but a very high correlation with Dd and Lo. The third component displays a very high correlation with Rr and Rh and a moderate correlation with S. The fourth component has a very high correlation with Rn and a high correlation with Dt. A total of 13 parameters were utilized in the morphometric analysis for prioritization; the PCA-based approach reduces the number of components from 13 to 4, as shown in Fig. 5, thereby saving computational time and assisting fluvial geomorphologists and hydrologists in selecting significant component weights (Meshram et al. 2019; Meshram and Sharma 2017). Normalization of each component indicates that PC2 carries the most weight at 0.3, followed by PC4 at 0.26, PC3 at 0.25, and PC1 at 0.2.

The matrix multiplication of the rotated matrix with their corresponding weights and the rank matrix of each parameter results in the prioritization of each sub-watershed, as shown in Table 10. The first rank is given to the sub-watershed with the lowest weighted average value, and vice versa. The average values range from 6.9 (WS8) to 26.9 (WS10), resulting in a priority rank of 1 for WS1 and 12 for WS10. Figure 6 illustrates a comprehensive map of prioritization using PCA.

GIUH based on the Nash model

The flow parameters of the GIUH model are evaluated using Eq. 1 to Eq. 12 as follows:

1. For sub-watershed 1

Bifurcation ratio (R_B) = 4.65, length ratio (R_L) = 0.56,

Main channel length (L) = 69615.35 m, mean slope (S_B) = 0.66

Highest order stream length (L_Ω) = 46.67, area ratio (R_A) = 0.70

Thus, velocity (v) $= 0.8562 L^{0.23} S_B^{0.385} = 0.8562 \times 69615.35^{0.23} \times 0.66^{0.385} = 9.478 \mathrm{m/s}$

Peak discharge (q_p) $= \left(\frac{1.31}{L_\Omega}\right) R_L^{0.43} v = \left(\frac{1.31}{46.67}\right) \times 0.56^{0.43} \times 9.48 = 0.207 \mathrm{inch/h}$

Time to peak (t_p) $= 0.44 \left(\frac{R_B}{R_A}\right)^{0.55} {R_L}^{-0.38} \frac{L_\Omega}{v} = 0.44 \times \left(\frac{4.65}{0.7}\right)^{0.55} \times 0.56^{-0.38} \times \frac{46.67}{9.478} = 7.691 \mathrm{h}$

Base time (t_b) $= 2/q_p = 2/0.207 = 9.67 \mathrm{h}$

Now, $\frac{(n-1)}{\Gamma(n)} \exp[-(n-1)](n-1)^{n-1} = 0.5764 \left(\frac{R_B}{R_A}\right)^{0.55} R_L^{0.05} = 0.5764 \times \left(\frac{4.65}{0.7}\right)^{0.55} \times 0.56^{0.05} = 1.591$

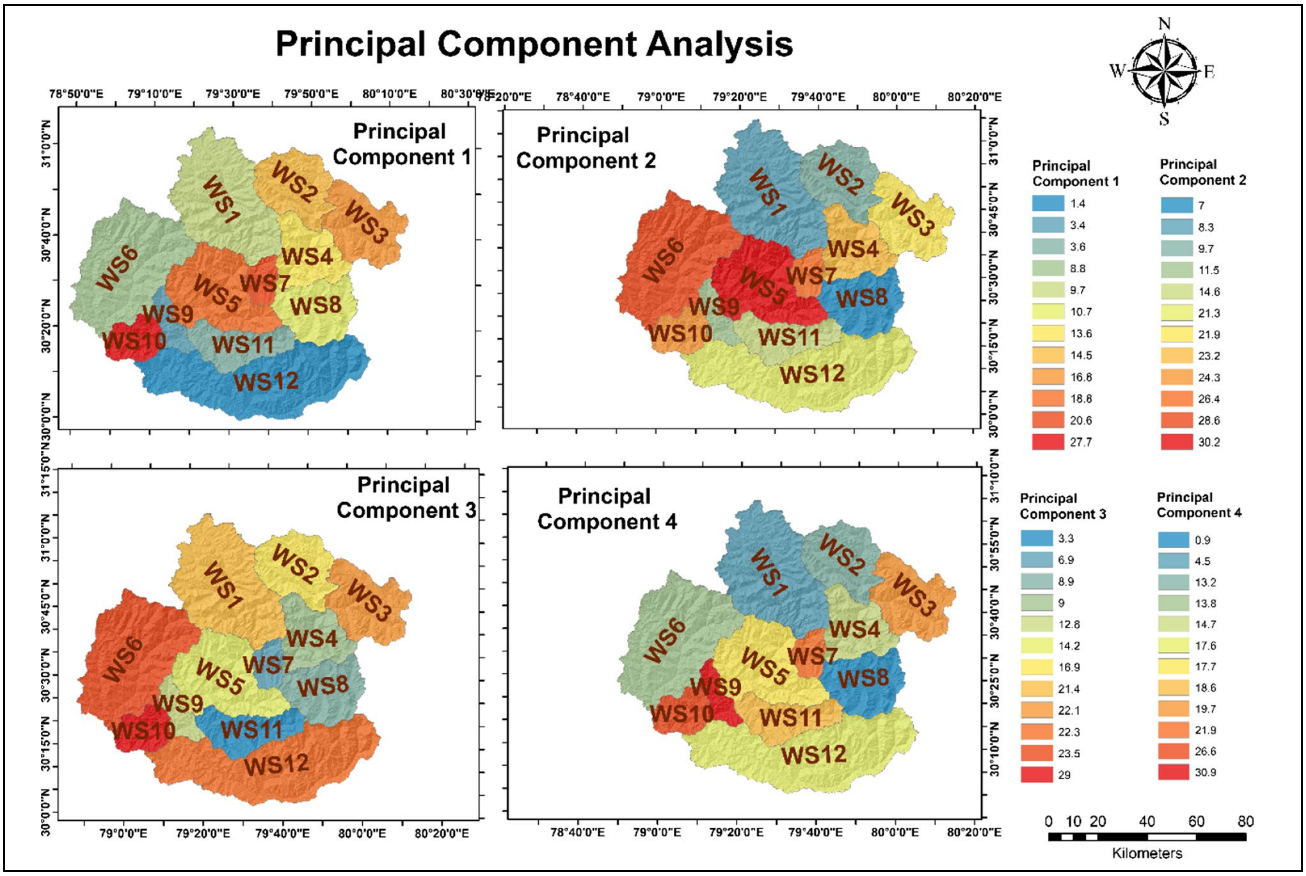

Fig. 5 The first four principal components map for each sub-watershed

Table 10 The sub-watershed prioritization map based on PCA approach

Sub-watershed	PC1 (0.2)	PC2 (0.3)	PC3 (0.25)	PC4 (0.26)	Weighted average	Priority
WS1	9.7	8.3	21.4	4.5	11.0	3
WS2	14.5	9.7	16.9	13.2	13.6	4
WS3	16.8	21.9	22.1	19.7	20.1	10
WS4	13.6	23.2	9.0	14.7	15.1	6
WS5	18.8	30.2	14.2	17.7	20.2	11
WS6	8.8	28.6	23.5	13.8	18.7	8
WS7	20.6	26.4	6.9	21.9	18.9	9
WS8	10.7	7.0	8.9	0.9	6.9	1
WS9	3.4	11.5	12.8	30.9	14.6	5
WS10	27.7	24.3	29.0	26.6	26.9	12
WS11	3.6	14.6	3.3	18.6	10.0	2
WS12	1.4	21.3	22.3	17.6	15.6	7

Solving for n gives $n = 17$

Hence, $k = 0.44\left(\frac{R_B}{R_A}\right)^{0.55} R_L^{0.05} \frac{1}{(n-1)} \frac{L_\Omega}{v} = 0.44 \times \left(\frac{4.65}{0.7}\right)^{0.55} \times 0.56^{0.05} \times \frac{1}{(17-1)} \times \frac{46.67}{9.478} = 0.481$

A similar approach is utilized to estimate these parameters for all the sub-watersheds, as shown in Table 11. The dynamic velocity varies from 7.335 m/s (WS7) to 10.761 m/s (WS12); q_p is the peak rainfall

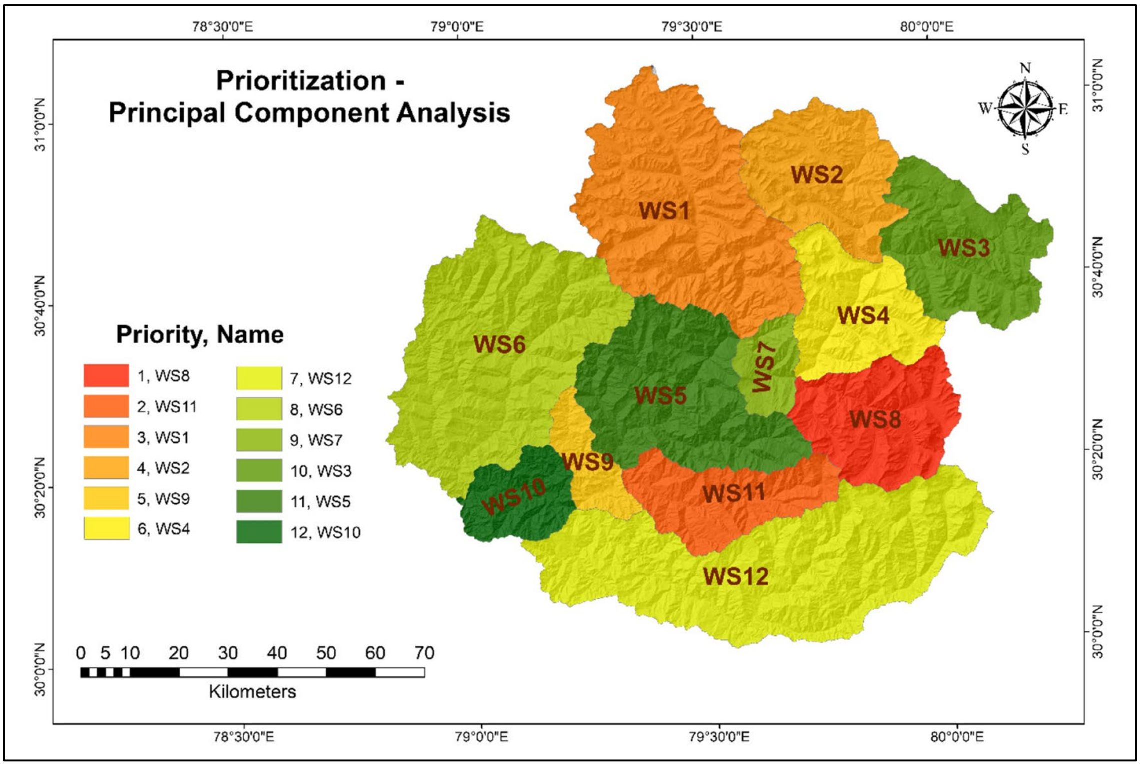

Fig. 6 The sub-watershed prioritization map based on PCA approach

intensity, which varies from 0.120 inch/h (WS12) to 1.034 inch/h (WS9); t_p varies from 1.453 h (WS9) to 12.315 h (WS12); t_b varies from 1.934 h (WS9) to 16.654 h (WS12); k varies from 0.102 (WS9) to 0.880 (WS12), and n varies from 11.3 (WS4) to 17.0 (WS1). These parameters are displayed in Fig. 7. These values are important in the hydrological modeling of watersheds that help predict the erosion potential of the sub-watersheds. The values are applied to prioritize sub-watersheds based on the assumption that high dynamic velocity and instantaneous peak magnify flash flood susceptibility, whereas a larger lag time and time to peak attenuate its impact. The resultant sub-watershed prioritization value obtained using GIUH is displayed in Table 12, and the map is shown in Fig. 8.

RUSLE approach

Table 13 offers information on the soil erosion rate and priority ranking of 12 sub-watersheds within the Alaknanda

Table 11 GIUH parameters as per the Nash model

Sub-watershed	Velocity (m/s)	q_p (inch/h)	tp (h)	tb	k	RHS of Eq. 11	n
WS1	9.478	0.207	7.691	9.670	0.481	1.591	17.0
WS2	8.668	0.350	4.000	5.716	0.320	1.400	13.5
WS3	8.318	0.470	3.180	4.257	0.226	1.494	15.1
WS4	9.450	0.446	2.852	4.486	0.277	1.271	11.3
WS5	9.235	0.362	4.214	5.522	0.285	1.526	15.8
WS6	9.509	0.973	1.545	2.055	0.108	1.504	15.3
WS7	7.335	0.840	1.572	2.382	0.142	1.320	12.1
WS8	8.612	0.353	3.774	5.672	0.337	1.331	12.2
WS9	7.872	1.034	1.453	1.934	0.102	1.502	15.3
WS10	8.033	0.292	4.816	6.839	0.382	1.408	13.6
WS11	9.050	0.203	6.458	9.837	0.587	1.313	12.0
WS12	10.761	0.120	12.315	16.654	0.880	1.479	15.0

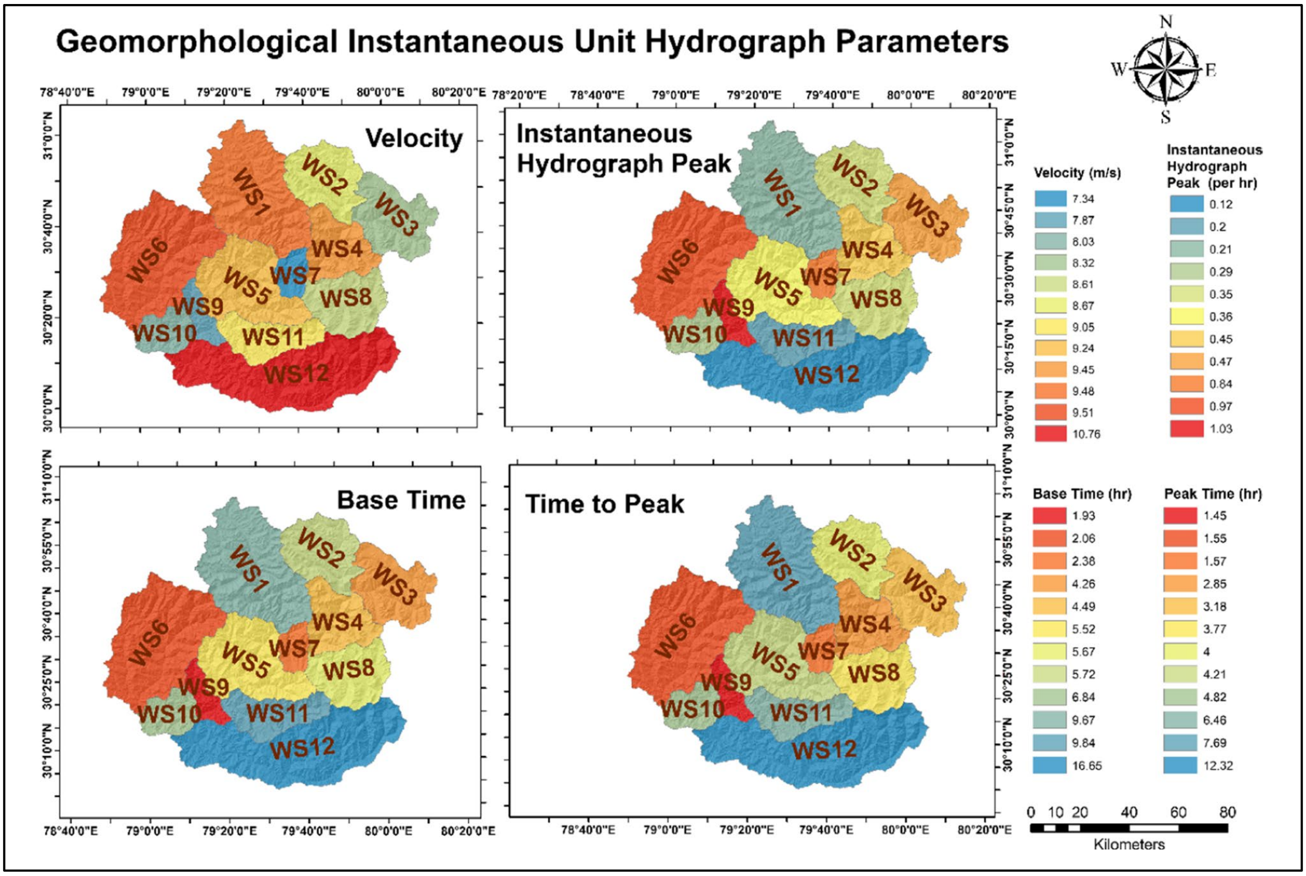

Fig. 7 The GIUH parameters map for each sub-watershed

Table 12 The sub-watershed prioritization map based on GIUH approach

Sub-watershed	Velocity (m/s)	qp (inch/h)	tp (h)	tb	Compound	Priority
WS1	3	10	11	10	8.5	9
WS2	7	8	7	8	7.5	8
WS3	9	4	5	4	5.5	5
WS4	4	5	4	5	4.5	3
WS5	5	6	8	6	6.25	6
WS6	2	2	2	2	2	1
WS7	12	3	3	3	5.25	4
WS8	8	7	6	7	7	7
WS9	11	1	1	1	3.5	2
WS10	10	9	9	9	9.25	10
WS11	6	11	10	11	9.5	12
WS12	1	12	12	12	9.25	10

watershed, as determined by the RUSLE model. The RUSLE model calculates soil erosion rates based on the product of five factors: the *R* factor, the *K* factor, the LS factor, the *C* factor, and the *P* factor, as well as the soil erosion rate. The *R* factor, which reflects rainfall erosivity, is the erosive force of rainfall, and it ranges between 294 (WS3) and 526 MJ mm/ha/h/year (WS12). A bigger *R* factor suggests a greater likelihood of soil erosion caused by intense rainfall. The *K* factor, which reflects soil erodibility, measures the soil's susceptibility to erosion, ranging from 0.042 t ha h/MJ/ha/mm (WS8) to 0.088 t ha h/MJ/ha/mm (WS9). Soil with a higher *K* factor is more susceptible to erosion. The LS factor, which measures the topographic effect on soil erosion, spans from a minimum of 1.3 (WS9 and WS10)

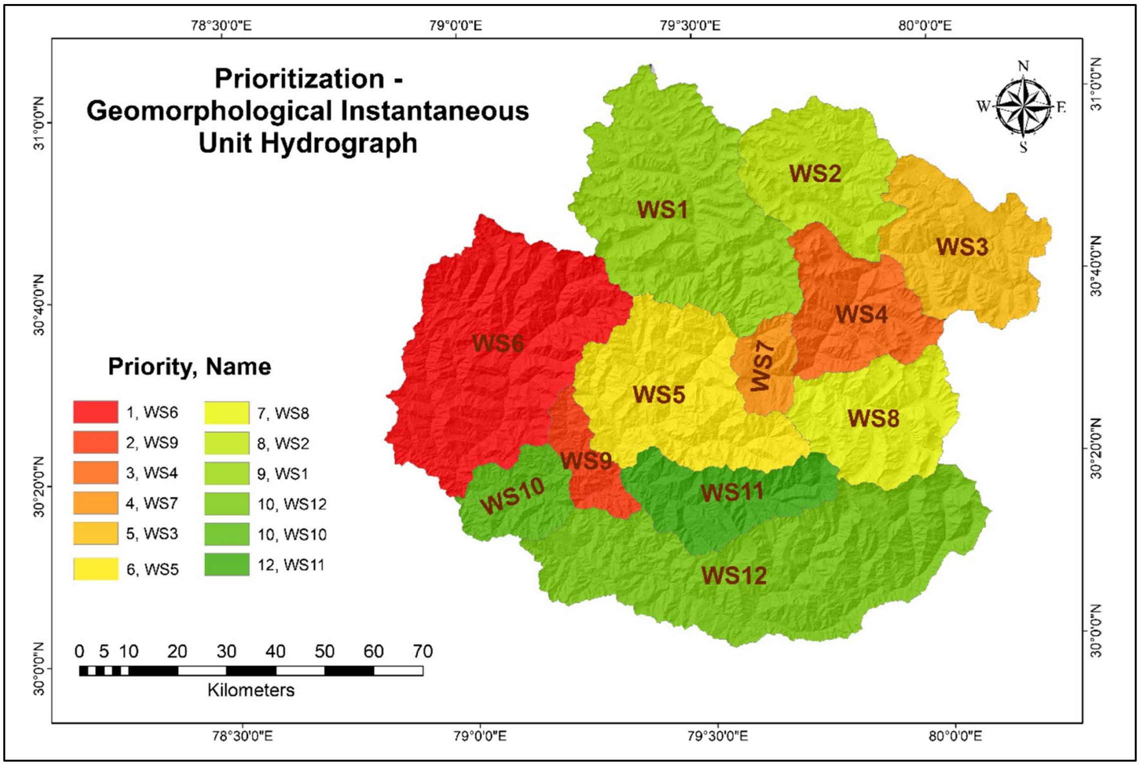

Fig. 8 The sub-watershed prioritization map based on GIUH approach

Table 13 The sub-watershed prioritization map based on RUSLE approach (Singh and Kansal 2023)

Sub-watershed	*R* factor (MJ mm / ha /h /year)	*K* factor (t ha h /MJ /ha /mm)	LS factor	*C* factor	*P* factor	Soil Erosion Rate (t /ha /year)	Priority
	Value	Value	Value	Value	Value	Value	
WS1	429	0.052	1.5	1	0.22	7.2	11
WS2	328	0.044	1.4	1.1	0.27	6	12
WS3	294	0.058	1.4	1.1	0.38	10.1	7
WS4	411	0.045	1.5	1	0.53	14.7	5
WS5	471	0.083	1.4	0.5	0.81	22	2
WS6	479	0.08	1.4	0.4	0.71	14.69	6
WS7	448	0.077	1.5	0.7	0.78	27.9	1
WS8	508	0.042	1.5	1.1	0.25	8.9	10
WS9	442	0.088	1.3	0.2	0.94	9.3	8
WS10	436	0.085	1.3	0.2	0.95	9.1	9
WS11	475	0.083	1.4	0.4	0.8	17.3	3
WS12	526	0.073	1.4	0.4	0.78	16.3	4

to a maximum of 1.5 (WS1, WS4, WS7, and WS8). Due to steeper slopes and longer slope lengths, a higher LS factor indicates a greater soil erosion risk. The *C* factor goes from a minimum of 0.2 (WS9 and WS10) to a maximum of 1.1 (WS2, WS3, and WS8) and depicts the land cover and management approach. A higher *C* factor suggests a lesser vegetation cover and a greater possibility for soil erosion. The *P* factor, which reflects the support practice, quantifies the influence of soil conservation practices on soil erosion and ranges from 0.22 (WS1) to 0.95(WS10). A lower *P* factor suggests more effective soil conservation methods and lower erosion risk. The projected soil erosion rate ranges from a minimum of 6 tons per hectare per year (WS2) to a high of 27.9 tons per year (WS7). Lastly, the sub-watersheds are sorted according to their soil erosion rate, with the sub-watershed with the greatest soil erosion rate (WS7) receiving the highest priority and the sub-watershed with the lowest soil erosion rate receiving the lowest priority (WS5). All the parameters are displayed in Fig. 9, and the sub-watershed prioritization map is shown in Fig. 10.

Comparative assessment of the individual and overall sub-watershed prioritization with the landslide and flash-flood inventories

A comparative analysis is conducted to evaluate the efficacy of the four different approaches to prioritization. The priority rankings are shown in ascending order, with the highest-priority sub-watershed receiving the lowest number and the lowest-priority sub-watershed receiving the highest number. According to the RUSLE approach, WS7 is ranked top priority, with WS5 and WS11 closely behind. On the other hand, the GIUH approach prioritizes WS6 as the most critical, with WS9 and WS4 being of secondary importance. Lastly, the CM approach designates WS8 as the highest priority, with WS1 and WS11 being the next in line. The PCA method identifies WS1 as having the highest priority, followed by WS8 and WS2.

The overall ranking of each sub-watershed is assessed through a weighted average methodology. The weighted average approach provides a more nuanced and customizable prioritization that considers the relative importance of different factors in determining sub-watershed priority (Kouli et al. 2014). By assigning different weights to each assessment method, stakeholders can focus on specific aspects of watershed management that are most relevant to their goals and objectives. Considering the average ranking of morphometric PCA and CM approaches, equal weightage was given to the morphometric, hydrological GIUH, and semi-empirical RUSLE techniques, as shown in Table 14. The overall priority indicates that sub-watersheds WS7, WS4, and WS6 require more urgent attention and resources to address their issues. These sub-watersheds have more significant erosion, flooding, or other environmental problems that must be mitigated to protect the surrounding ecosystem and communities. The observations are also validated from the landslides and flash-flood inventories depicting 264 landslides and 8 flash-flood incidents. The sub-watersheds WS9, WS8, WS11, WS5, and WS12 still require attention and resources, but the urgency is lower than the higher priority sub-watersheds. These sub-watersheds exhibit moderate environmental issues that can be effectively addressed through targeted interventions and regular monitoring activities. Furthermore, landslides are observed in these sub-watersheds at approximately 483 incidents, with an additional 19 flash-flood events. This information suggests that these sub-watersheds may benefit from focused interventions to mitigate the frequency and severity of environmental risks and hazards to safeguard the surrounding ecosystem and communities. The sub-watersheds WS1, WS3, WS2, and WS10 exhibit a relatively lower level of environmental issues and are considered less critical regarding watershed management. Nevertheless, these sub-watersheds should still undergo regular monitoring and management practices to prevent the occurrence of environmental hazards in the future. Additionally, the frequency of observed landslides in these sub-watersheds is estimated to be approximately 176 incidents, with a further 2 flash-flood events recorded. The combined sub-watershed prioritization map is shown in Fig. 11. The results indicate that the effectiveness of each method varied for each sub-watershed. Thus, it is crucial to have a well-informed decision-making process considering each sub-watershed's specific conditions. Depending on the prevailing conditions, this insight aids in selecting the most efficient strategy for mitigating risks, safeguarding communities, and preserving infrastructure from the detrimental impacts of flash floods and associated landslides and erosions.

Discussions

This paper attempts to compare the morphometric PCA and CM, GIUH, and RUSLE methods for sub-watershed prioritization and estimate the overall priority of the sub-watershed. The morphometric approach focuses on the topography and shape of the catchment area (Arnous and Omar 2018; Das et al. 2021). It prioritizes sub-watersheds using slope, drainage density, and relief ratio metrics. This approach helps identify areas with a higher potential for landslides (Carrara et al. 1995; Jiménez-Perálvarez et al. 2009; Martha et al. 2010). The GIUH method, on the other hand, considers the catchment response based on the characteristics of the hydrograph, including velocity, peak discharge, time to peak, and base time (Rai et al. 2009; Sorman 1995). This approach provides a more accurate representation of the catchment response and is useful for identifying areas likely to be impacted by flash floods (Khaleghi et al. 2014; Kumar et al. 2007; Sahoo and Jain 2018). The RUSLE model calculates soil erosion by evaluating factors such as rainfall erosivity, soil erodibility, slope dynamics, cover management, and conservation practices, providing a comprehensive estimation of erosion under varying conditions (Bhattacharya et al. 2021; Fayas et al. 2019; George et al. 2021). By integrating the four techniques, a holistic watershed perspective emerges, enhancing the understanding of hydrological processes, soil erosion, landform traits, and land cover management. This insight guides informed decisions for watershed conservation and sustainable development.

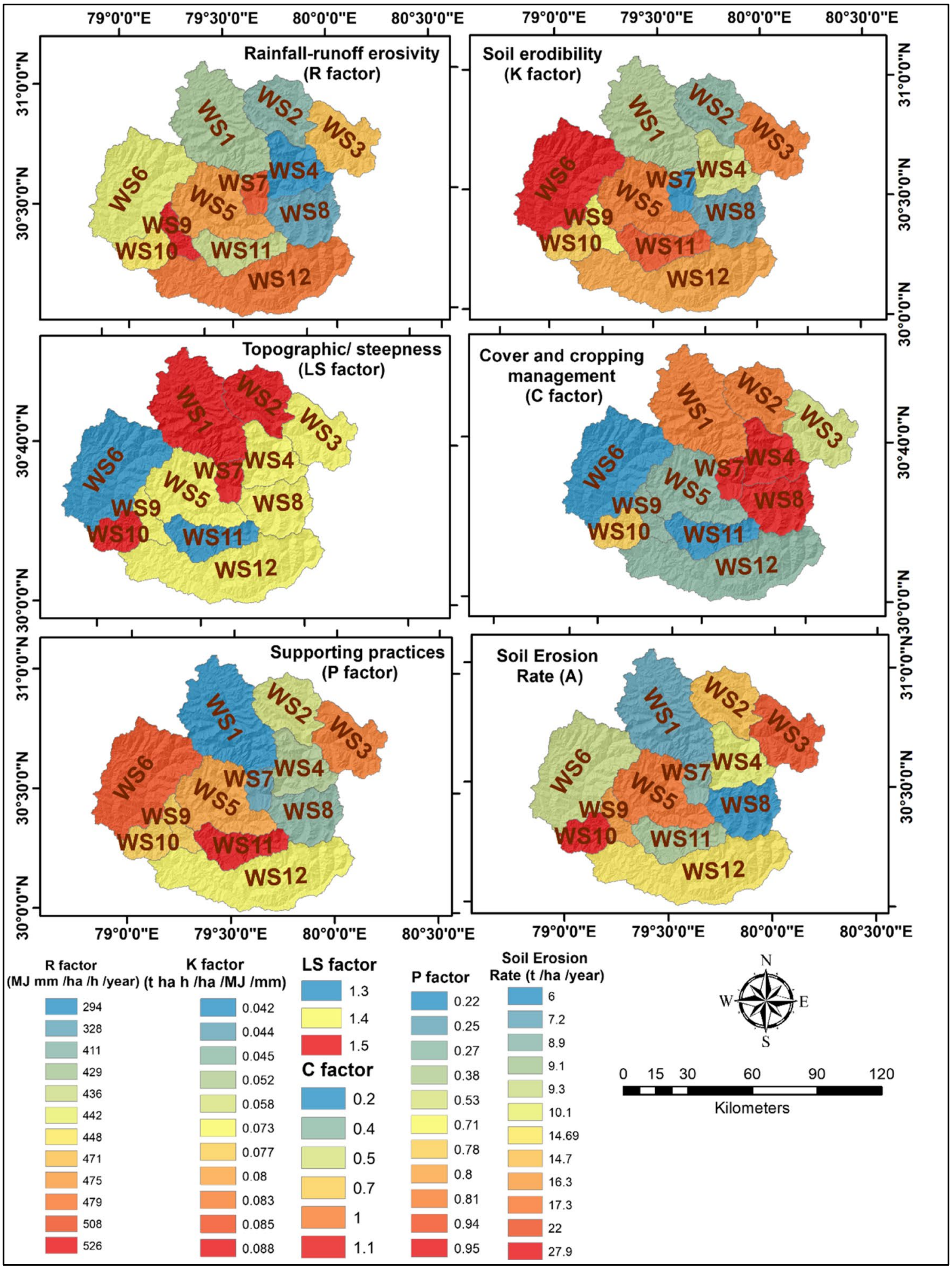

Fig. 9 The RUSLE parameters map for each sub-watershed

The results of this research are evident in the classification of sub-watersheds pertaining to flash flood-induced landslides. The overall priority rankings, which categorized the sub-watersheds into three main categories, are drawn from an intricate analysis of landslide frequency, flash-flood incidents, and historical erosional patterns. These could be summarized as follows:

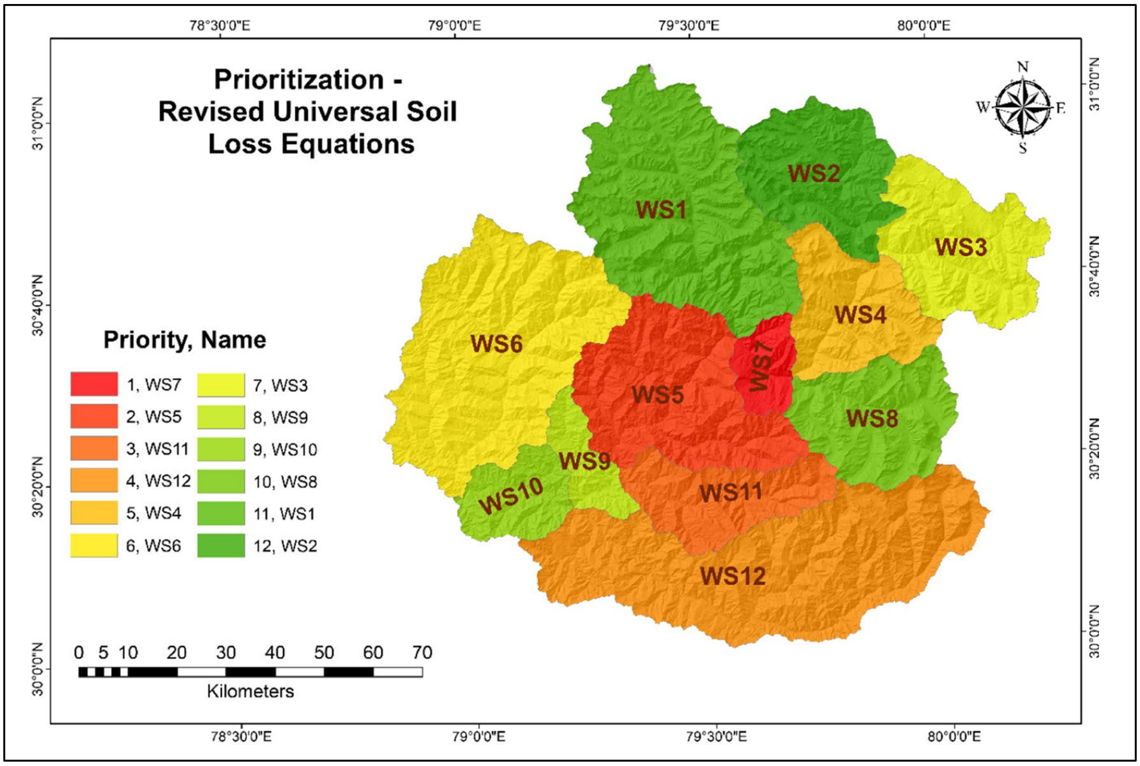

Fig. 10 The sub-watershed prioritization map based on RUSLE approach

Table 14 Overall sub-watershed prioritization

Sub-watershed no	CM Priority	PCA Priority	GIUH Priority	RUSLE Priority	Weighted average	Overall Priority
WS1	2	3	9	11	7.5	9
WS2	4	4	8	12	8.0	11
WS3	12	10	5	7	7.7	10
WS4	6	6	3	5	4.7	2
WS5	10	11	6	2	6.2	7
WS6	9	8	1	6	5.4	4
WS7	8	9	4	1	4.4	1
WS8	1	1	7	10	6.0	6
WS9	7	5	2	8	5.3	3
WS10	11	12	10	9	10.2	12
WS11	3	2	12	3	5.8	5
WS12	5	7	10	4	6.7	8

Category I (high priority): Sub-watersheds WS7, WS4, WS9, and WS6 fall under this category. These areas displayed significant signs of erosion and flooding. For instance, WS9, influenced heavily by its unique topographical characteristics, witnessed enhanced runoff, while WS6's susceptibility is amplified by the region's consistent heavy rainfall events, pushing its erosivity index higher. Specifically, WS6 recorded 244 landslides and 7 flash-flood incidents, depicting a watershed under consistent environmental stress. W7, W6, and WS4 are also characterized by very high soil erosion rates.

Category II (moderate attention): Sub-watersheds like WS11, WS8, WS5, and WS12, although not as severely impacted as the first category, still showcased vulnerabilities. These regions recorded moderate erosional traits but also hinted at upcoming potential risks if not addressed. WS12, for instance, had a higher rainfall erosivity and a history of rapid hydrological flow characteristics and landslide

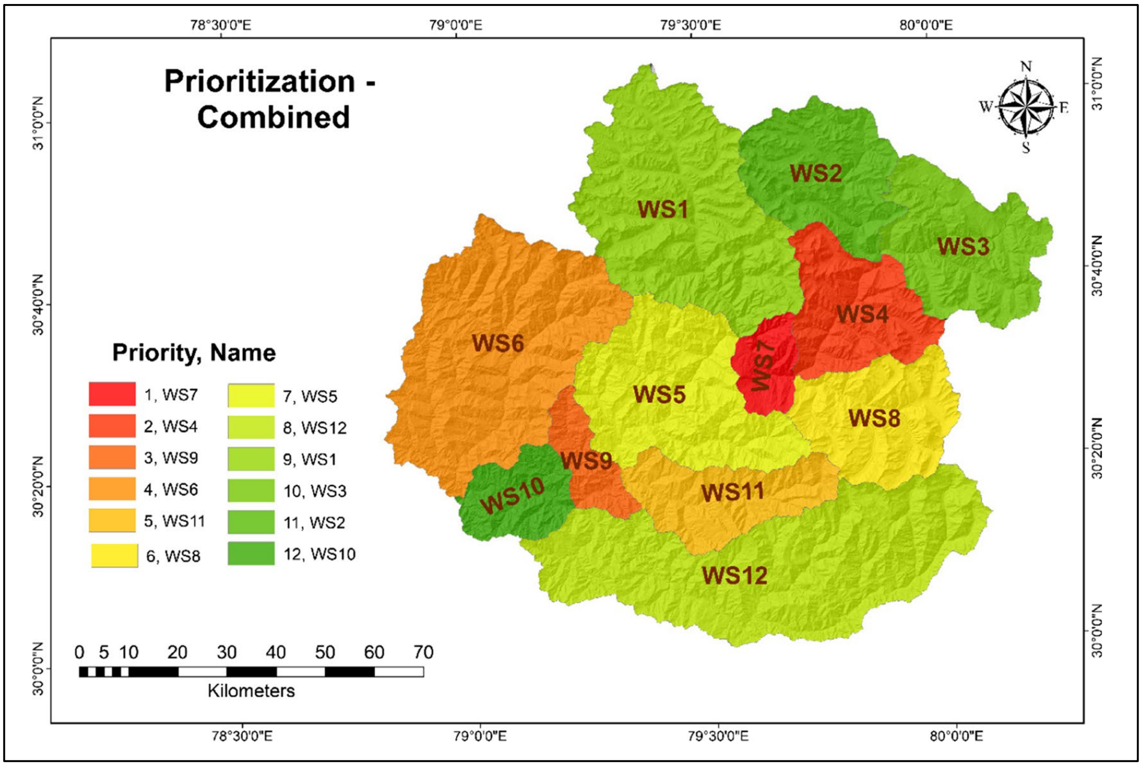

Fig. 11 The sub-watershed prioritization map based on weighted average approach

incidents. WS5, WS11, and WS12 demonstrated higher soil erosion rates.

Category III (regular monitoring): This group, including WS1, WS3, WS2, and WS10, presented lesser erosional characteristics but suggested underlying vulnerabilities that could escalate if left unchecked. While WS10 is presently stable, certain regions within it possess soil types susceptible to accelerated erosion because of 160 landslide incidents, warranting consistent monitoring.

To validate our findings, field surveys were undertaken (Fig. 12). Detailed photographs, damaged area coordinates, and local narratives confirmed our computational assessments, emphasizing the need for strategic interventions tailored for each category. The results showed that the areas with the highest impact were also located within the high-priority sub-basins, indicating the validity of the computed findings. The current situation also indicates the need for suitable mitigation strategies against flash-flood disasters in the Himalayan watersheds. The resulting landslides and induced erosion negatively impact agricultural productivity and cause downstream sedimentation, decreasing reservoir storage, and increasing flood risks.

While this study offers a comprehensive and integrative analysis of flash flood-induced landslides in the Alaknanda River basin, several limitations should be noted. The inherent assumptions of the utilized methods, PCA, CM, GIUH, and RUSLE, may not always mirror the intricate real-world scenarios, especially as RUSLE assumes steady-state conditions and the accuracy of results depends on the fidelity of input datasets. The findings are specific to a part of the Indian Himalayan Region, but there is an underlying assumption that they might apply to other regions. However, unaccounted anthropogenic and climatic factors can influence vulnerability assessments.

Conclusions

This study intricately juxtaposed four methodologies—morphometric PCA, morphometric combined (CM), Geomorphic Instantaneous Unit Hydrograph (GIUH), and Revised Universal Soil Loss Equation (RUSLE)—to discern the most suitable approach to sub-watershed prioritization concerning flash flood-induced landslides. Leveraging the insights from morphometric analysis, the profound influence of topographical nuances on potential landslide zones became evident. The GIUH method provided a granular perspective on hydrological aspects, especially highlighting vulnerabilities to flash floods.

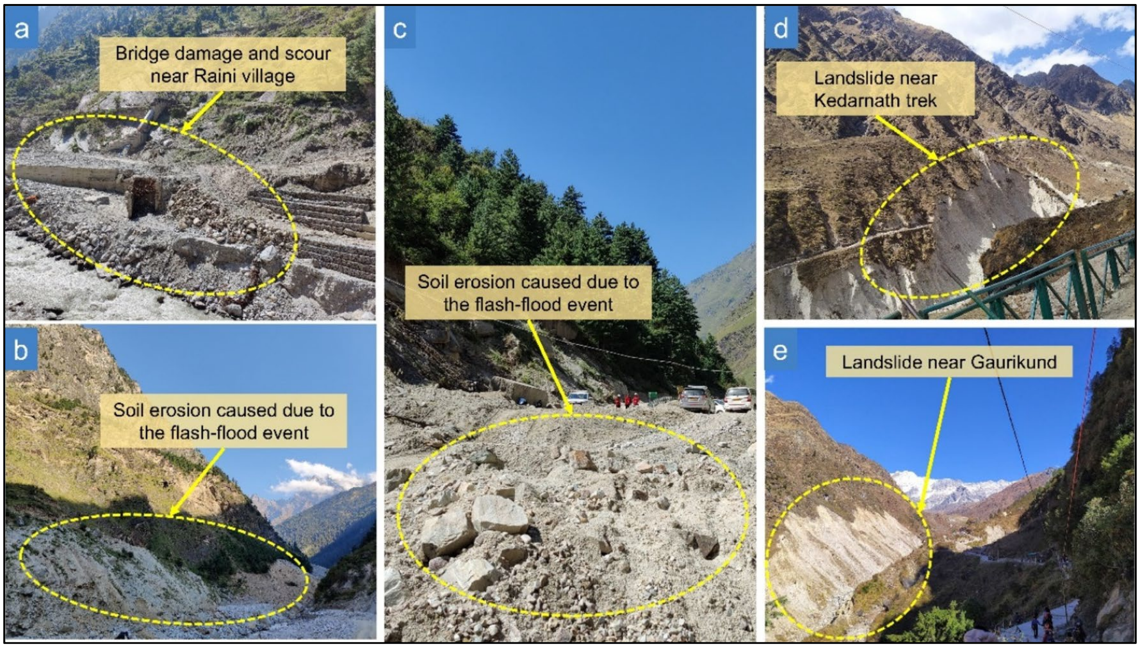

Fig. 12 Field survey photographs (October 2020 and 2021): **a** A damaged site close to the bridge in Raini village (WS7). **b** A flash flood eroded area in WS5. **c** An eroded upstream section of the Alaknanda River (WS8). **d** Flash flood induced landslides in Kedarnath (WS6). **e** Landslides and erosion near Gaurikund (WS6)

Additionally, the RUSLE model illuminated the intricacies of erosion dynamics. With the confluence of these methods, distinct vulnerability categories emerged: Category I (high priority) encapsulates WS7, WS4, WS9, and WS6. Most notably, WS6 endured a staggering 244 landslides and 7 flash-flood incidents. Category II (moderate attention) includes WS11, WS8, WS5, and WS12. To illustrate, WS12's hydrological traits indicate potential vulnerabilities due to landslides. Category III (regular monitoring) comprises WS1, WS3, WS2, and WS10. For instance, WS10, although presently modeled as stable, exhibits 160 landslide incidents. Validation exercises through field surveys reinforced these computational conclusions, with the most impacted regions aligning with high-priority basins. However, it is essential to underscore that while this research presents a comprehensive view of the Alaknanda River basin, the methods' inherent assumptions might not capture all real-world complexities. Even though the insights are tailored to a segment of the Indian Himalayan Region, the possibility of extrapolating them to other areas exists. Nevertheless, unforeseen anthropogenic and climatic deviations could alter the vulnerability landscape. These findings necessitate stakeholders to craft mitigation strategies that holistically cater to each watershed's distinct attributes, championing ecosystem preservation and community well-being.

Supplementary Information The online version contains supplementary material available at https://doi.org/10.1007/s11356-023-30613-6.

Acknowledgements The authors express their gratitude to the Indian Institute of Technology, Roorkee, for their provision of essential infrastructure and support, enabling the successful completion of this research. Additionally, the authors extend their appreciation to the National Institute of Hydrology, Roorkee, for their assistance during the field surveys. The authors would also like to acknowledge the contributions of scientists affiliated with Environmental Systems Research Institute (ESRI), Google Earth Engine, Google Earth, who generously provided topographic data and high-resolution base layers.

Author contribution All authors contributed to the current research. Manuscript preparation was performed by S. S. The data collections and field survey were carried out by M. L. K. The analysis was performed by S. S. and M. L. K. All authors read and approved the final manuscript.

Data availability The information about the data, resolution/scale, purpose, and source data that support the findings of this study are described in "Datasets and tools" section of the manuscript.

Declarations

Ethics approval This study did not involve human or animal subjects and therefore did not require ethical approval.

Consent to participate Not applicable, as this study did not involve human subjects.

Consent for publication All authors of this manuscript agree to its publication.

Competing interests The authors declare no known competing interests.

References

Abdeta GC, Tesemma AB, Tura AL, Atlabachew GH (2020) Morphometric analysis for prioritizing sub-watersheds and management planning and practices in Gidabo Basin, Southern Rift Valley of Ethiopia. Appl Water Sci 10(7):158. https://doi.org/10.1007/s13201-020-01239-7

Agarwal CS (1998) Study of drainage pattern through aerial data in Naugarh area of Varanasi district, U.P. J Indian Soc Remote Sens 26(4):169–175. https://doi.org/10.1007/BF02990795

Aher PD, Adinarayana J, Gorantiwar SD (2014) Quantification of morphometric characterization and prioritization for management planning in semi-arid tropics of India: a remote sensing and GIS approach. J Hydrol 511:850–860. https://doi.org/10.1016/j.jhydrol.2014.02.028

Arnous MO, Omar AE (2018) Hydrometeorological hazards assessment of some basins in Southwestern Sinai area, Egypt. J Coast Conserv 1–23. https://doi.org/10.1007/s11852-018-0604-2

Azmeri L, Hadihardaja IK, Vadiya R (2016) Identification of flash flood hazard zones in mountainous small watershed of Aceh Besar Regency, Aceh Province, Indonesia. Egypt J Remote Sens Space Sci 19(1):143–160. https://doi.org/10.1016/j.ejrs.2015.11.001

Bamufleh S, Al-Wagdany A, Elfeki A, Chaabani A (2020) Developing a geomorphological instantaneous unit hydrograph (GIUH) using equivalent Horton-Strahler ratios for flash flood predictions in arid regions. Geomat Nat Haz Risk 11(1):1697–1723. https://doi.org/10.1080/19475705.2020.1811404

Batar AK, Watanabe T (2021) Landslide susceptibility mapping and assessment using geospatial platforms and weights of evidence (WoE) method in the Indian Himalayan Region: recent developments, gaps, and future directions. ISPRS Int J Geo Inf 10(3):114. https://doi.org/10.3390/ijgi10030114

Beg Ayad Ali Faris (2015) Morphometric toolbox: a new technique in basin morphometric analysis using ArcGIS. Glob J Earth Sci Eng 2(2):21–30. https://doi.org/10.15377/2409-5710.2015.02.02.1

Bhat SU, Islam ST, Sabha I, Khanday SA (2022) Understanding morphometric response to erosion and flash floods in Jhelum River basin: index-based geospatial management approach. Int J Environ Sci Technol 19(10):10157–10175. https://doi.org/10.1007/s13762-021-03701-8

Bhattacharya RK, Chatterjee Das N, Acharya P, Das K (2021) Morphometric analysis to characterize the soil erosion susceptibility in the western part of lower Gangetic River basin, India. Arab J Geosci 14(6). https://doi.org/10.1007/s12517-021-06819-8

Bhattacharyya R, Ghosh B, Mishra P, Mandal B, Rao C, Sarkar D, Das K, Anil K, Lalitha M, Hati K, Franzluebbers A (2015) Soil degradation in india: challenges and potential solutions. Sustainability 7(4):3528–3570. https://doi.org/10.3390/su7043528

Biswas B, Vignesh KS, Ranjan R (2021) Landslide susceptibility mapping using integrated approach of multi-criteria and geospatial techniques at Nilgiris district of India. Arab J Geosci 14(11):980. https://doi.org/10.1007/s12517-021-07341-7

Budakoti S, Singh C, Pal PK (2019) Assessment of various cumulus parameterization schemes for the simulation of very heavy rainfall event based on optimal ensemble approach. Atmos Res 218(April 2018):195–206. https://doi.org/10.1016/j.atmosres.2018.12.005

Carrara A, Cardinali M, Guzzetti F, Reichenbach P (1995) Gis Technology in Mapping Landslide Hazard 135–175. https://doi.org/10.1007/978-94-015-8404-3_8

Chandniha SK, Kansal ML (2017) Prioritization of sub-watersheds based on morphometric analysis using geospatial technique in Piperiya watershed, India. Appl Water Sci 7(1):329–338. https://doi.org/10.1007/s13201-014-0248-9

Choudhari PP, Nigam GK, Singh SK, Thakur S (2018) Morphometric based prioritization of watershed for groundwater potential of Mula river basin, Maharashtra, India. Geol Ecol Landsc 2(4):256–267. https://doi.org/10.1080/24749508.2018.1452482

Costache R, Hong H, Pham QB (2020) Comparative assessment of the flash-flood potential within small mountain catchments using bivariate statistics and their novel hybrid integration with machine learning models. Sci Total Environ 711:134514. https://doi.org/10.1016/j.scitotenv.2019.134514

Cudennec C, Fouad Y, Gatot IS, Duchesne J (2004) A geomorphological explanation of the unit hydrograph concept. Hydrol Process 18(4):603–621. https://doi.org/10.1002/hyp.1368

Das B, Paul A, Bordoloi R, Tripathi OP, Pandey PK (2018) Soil erosion risk assessment of hilly terrain through integrated approach of RUSLE and geospatial technology: a case study of Tirap District, Arunachal Pradesh. Model Earth Syst Environ 4(1):373–381. https://doi.org/10.1007/s40808-018-0435-z

Das B, Singh S, Jain SK, Thakur PK (2021) prioritization of subbasins of Gomti River for soil and water conservation through morphometric and LULC analysis using remote sensing and GIS. J Indian Soc Remote Sens 49(10):2503–2522. https://doi.org/10.1007/s12524-021-01410-w

Das B, Bordoloi R, Thungon LT, Paul A, Pandey PK, Mishra M, Tripathi OP (2020) An integrated approach of GIS, RUSLE and AHP to model soil erosion in West Kameng watershed, Arunachal Pradesh. J Earth Syst Sci 129(1). https://doi.org/10.1007/s12040-020-1356-6

Dimri AP, Thayyen RJ, Kibler K, Stanton A, Jain SK, Tullos D, Singh VP (2016) A review of atmospheric and land surface processes with emphasis on flood generation in the Southern Himalayan rivers. Sci Total Environ 556:98–115. https://doi.org/10.1016/j.scitotenv.2016.02.206

Dubey RK, Jha VN (2022) Soil erosion evaluation through prioritization of Shyok-Nubra Watershed using morphometric, principal component and weighted sum approaches. PREPRINT (Version 1) available at Research Square. https://doi.org/10.21203/rs.3.rs-1922043/v1

Dutta D, Das S, Kundu A, Taj A (2015) Soil erosion risk assessment in Sanjal watershed, Jharkhand (India) using geo-informatics, RUSLE model and TRMM data. Model Earth Syst Environ 1(4):1–9. https://doi.org/10.1007/s40808-015-0034-1

Duulatov E, Pham QB, Alamanov S, Orozbaev R, Issanova G, Asankulov T (2021) Assessing the potential of soil erosion in Kyrgyzstan based on RUSLE, integrated with remote sensing. Environ Earth Sci 80(18):1–13. https://doi.org/10.1007/s12665-021-09943-6

Fairfield J, Leymarie P (1991) Drainage networks from grid digital elevation models. Water Resour Res 27(5):709–717. https://doi.org/10.1029/90WR02658

Farhan Y, Anaba O, Salim A (2016) Morphometric analysis and flash floods assessment for drainage basins of the Ras En Naqb Area, South Jordan Using GIS. J Geosci Environ Prot 04(06):9–33. https://doi.org/10.4236/gep.2016.46002

Fayas CM, Abeysingha NS, Nirmanee KGS, Samaratunga D, Mallawatantri A (2019) Soil loss estimation using rusle model to prioritize erosion control in KELANI river basin in Sri Lanka. Int Soil Water Conserv Res 7(2):130–137. https://doi.org/10.1016/j.iswcr.2019.01.003

Ganasri BP, Ramesh H (2016) Assessment of soil erosion by RUSLE model using remote sensing and GIS - a case study of Nethravathi Basin. Geosci Front 7(6):953–961. https://doi.org/10.1016/j.gsf.2015.10.007

Gayen A, Pourghasemi HR, Saha S, Keesstra S, Bai S (2019) Gully erosion susceptibility assessment and management of hazard-prone areas in India using different machine learning algorithms. Sci Total Environ 668:124–138. https://doi.org/10.1016/j.scitotenv.2019.02.436

George J, Kumar S, Hole RM (2021) Geospatial modelling of soil erosion and risk assessment in Indian Himalayan region—a study of Uttarakhand state. Environ Adv 4(August 2020):100039. https://doi.org/10.1016/j.envadv.2021.100039

Gharibreza M, Bahrami Samani A, Arabkhedri M, Zaman M, Porto P, Kamali K, Sobh-Zahedi S (2021) Investigation of on-site implications of tea plantations on soil erosion in Iran using 137Cs method and RUSLE. Environ Earth Sci 80(1):1–14. https://doi.org/10.1007/s12665-020-09347-y

Gupta VK, Waymire E, Wang CT (1980) A representation of an instantaneous unit hydrograph from geomorphology. Water Resour Res 16(5):855–862. https://doi.org/10.1029/WR016i005p00855

Halder S, Roy MB, Roy PK (2021) Modelling soil erosion risk of a tropical plateau basin to identify priority areas for conservation. Environ Earth Sci 80(18):1–24. https://doi.org/10.1007/s12665-021-09941-8

Horton RE (1932) Drainage-basin characteristics. Trans Am Geophys Union 13(1):350. https://doi.org/10.1029/TR013i001p00350

Horton RE (1945) Erosional development of streams and their drainage basins; hydrophysical approach to quantitative morphology. Bull Geol Soc Am 56(March):275–370

Horton P, Jaboyedoff M, Zimmermann M, Mazotti B, Longchamp C (2011) Flow-R, a model for debris flow susceptibility mapping at a regional scale - some case studies. Proceedings of the 5th International Conference on Debris-Flow Hazards Mitigation: Mechanics, Prediction and Assessment 875–884. https://doi.org/10.4408/IJEGE.2011-03.B-095

Hydrologic Engineering Center. HEC-HMS User's Manual version 4.7. Selecting a discretization method. Retrieved May 18, 2023, from https://www.hec.usace.army.mil/confluence/hmsdocs/hmsum/4.7/subbasin-elements/selecting-a-discretizationmethod

Jiménez-Perálvarez JD, Irigaray C, El Hamdouni R, Chacón J (2009) Building models for automatic landslide-susceptibility analysis, mapping and validation in ArcGIS. Nat Hazards 50(3):571–590. https://doi.org/10.1007/s11069-008-9305-8

Joshi M, Kumar P, Sarkar P (2021) Morphometric parameters based prioritization of a Mid-Himalayan watershed using fuzzy analytic hierarchy process. E3S Web Conf 280:10004. https://doi.org/10.1051/e3sconf/202128010004

Kansal ML, Singh S (2022) Flood management issues in hilly regions of Uttarakhand (India) under changing climatic conditions. Water 14(12). https://doi.org/10.3390/w14121879

Khaleghi MR, Ghodusi J, Ahmadi H (2014) Regional analysis using the geomorphologic instantaneous unit hydrograph (GIUH) method. Soil Water Res 9(1):25–30. https://doi.org/10.17221/33/2012-swr

Kouli M, Loupasakis C, Soupios P, Rozos D, Vallianatos F (2014) Landslide susceptibility mapping by comparing the WLC and WofE multi-criteria methods in the West Crete Island, Greece. Environ Earth Sci 72(12):5197–5219. https://doi.org/10.1007/s12665-014-3389-0

Kumar R, Chatterjee C, Singh RD, Lohani AK, Kumar S (2007) Runoff estimation for an ungauged catchment using geomorphological instantaneous unit hydrograph (GIUH) models. Hydrol Process 21(14):1829–1840. https://doi.org/10.1002/hyp.6318

Kumar P, Sarkar P (2022) A comparison of the AHP and TOPSIS multi-criteria decision-making tools for prioritizing subwatersheds using morphometric parameters' analysis. Model Earth Syst Environ 0123456789. https://doi.org/10.1007/s40808-021-01334-x

Madiona RMT, Winkler DA, Muir BW, Pigram PJ (2019) Optimal machine learning models for robust materials classification using ToF-SIMS data. Appl Surf Sci 487(March):773–783. https://doi.org/10.1016/j.apsusc.2019.05.123

Martha TR, Kerle N, Jetten V, van Westen CJ, Kumar KV (2010) Characterising spectral, spatial and morphometric properties of landslides for semi-automatic detection using object-oriented methods. Geomorphology 116(1–2):24–36. https://doi.org/10.1016/j.geomorph.2009.10.004

Maury S, Gholkar M, Jadhav A, Rane N (2019) Geophysical evaluation of soils and soil loss estimation in a semi-arid region of Maharashtra using revised universal soil loss equation (RUSLE) and GIS methods. Environ Earth Sci 78(5):1–15. https://doi.org/10.1007/s12665-019-8137-z

Melton MA (1957) An analysis of the relations among elements of climate, surface properties, and geomorphology. Office of Naval Research Technical Report No. 11, vol 11, p 99

Meraj G, Romshoo SA, Yousuf AR, Altaf S, Altaf F (2015) Assessing the influence of watershed characteristics on the flood vulnerability of Jhelum basin in Kashmir Himalaya. Nat Hazards 77(1):153–175. https://doi.org/10.1007/s11069-015-1605-1

Meshram SG, Sharma SK (2017) Prioritization of watershed through morphometric parameters: a PCA-based approach. Appl Water Sci 7(3):1505–1519. https://doi.org/10.1007/s13201-015-0332-9

Meshram SG, Alvandi E, Singh VP, Meshram C (2019) Comparison of AHP and fuzzy AHP models for prioritization of watersheds. Soft Comput 23(24):13615–13625. https://doi.org/10.1007/s00500-019-03900-z

Miller V (1953) A quantitative geomorphic study of drainage basin characteristics in the clinch mountain area, Virginia and Tennessee. Project NR 389-402, Technical Report 3, Columbia University, Department of Geology, ONR, New York

Mishra PK, Thayyen RJ, Singh H, Das S, Nema MK, Kumar P (2022) Assessment of cloudbursts, extreme rainfall and vulnerable regions in the Upper Ganga basin, Uttarakhand. India. Int J Disaster Risk Reduct 69(December 2021):102744. https://doi.org/10.1016/j.ijdrr.2021.102744

Moore ID, Burch GJ (1986) Modelling erosion and deposition: topographic effects. Trans Am Soc Agric Eng 29(6):1624–1630. https://doi.org/10.13031/2013.30363

Nongthombam J, Choudhury P, Ullah N, Singh KV (2011) A Geomorphological based rainfallrunoff model for ungauged watersheds. Int J Geom Geosci 2:676–687

Nookaratnam K, Srivastava YK, Venkateswara Rao V, Amminedu E, Murthy KSR (2005) Check dam positioning by prioritization micro-watersheds using SYI model and morphometric analysis - remote sensing and GIS perspective. J Indian Soc Remote Sens 33(1):25–38. https://doi.org/10.1007/BF02989988

Pandey VK, Mishra A (2021) Causes and disaster risk reduction measures for hydrometerological disaster in Uttarakhand, India. Emerg Challenges Environ Earth Sci 1(2):99–118. https://doi.org/10.9734/bpi/ecees/v1/1617a

Panwar S, Khan MYA, Chakrapani GJ (2016) Grain size characteristics and provenance determination of sediment and dissolved load of Alaknanda River, Garhwal Himalaya, India. Environ Earth Sci 75(2):1–15. https://doi.org/10.1007/s12665-015-4785-9

Panwar S, Agarwal V, Chakrapani GJ (2017) Morphometric and sediment source characterization of the Alaknanda river basin, headwaters of river Ganga. Nat Hazards 87(3):1649–1671. https://doi.org/10.1007/s11069-017-2838-y

Patel DP, Srivastava PK (2013) Flood hazards mitigation analysis using remote sensing and GIS: correspondence with town planning scheme. Water Resour Manag 27(7):2353–2368. https://doi.org/10.1007/s11269-013-0291-6

Pathare JA, Pathare AR (2021) Watershed prioritization for soil and water conservation in Darna River basin: a PCA approach. Sustain Water Resour Manag 7(4):1–15. https://doi.org/10.1007/s40899-021-00531-x

Rahaman SA, Ajeez SA, Aruchamy S, Jegankumar R (2015) Prioritization of sub watershed based on morphometric characteristics using fuzzy analytical hierarchy process and geographical information system – a study of Kallar watershed, Tamil Nadu. Aquatic

Procedia 4(Icwrcoe):1322–1330. https://doi.org/10.1016/j.aqpro.2015.02.172

Rai RK, Upadhyay A, Sarkar S, Upadhyay AM, Singh VP (2009) GIUH based transfer function for Gomti River basin of India. J Spat Hydrol 9(2):29–50

Rai PK, Mohan K, Mishra S, Ahmad A, Mishra VN (2017) A GIS-based approach in drainage morphometric analysis of Kanhar River Basin, India. Appl Water Sci 7(1):217–232. https://doi.org/10.1007/s13201-014-0238-y

Rathore CS, Singh M, Kothari M, Yadav KK (2022) Morphometric analysis of Bhesra Kalan micro-watershed using remote sensing and GIS technique. Indian J Ecol 154–159. https://doi.org/10.55362/ije/2022/3495

Renard K, Foster G, Weesies G, McCool D, Yoder D (1997) Predicting soil erosion by water: a guide to conservation planning with the revised universal soil loss equation (RUSLE). US Department of Agriculture, Agriculture Handbook No.703USDA, USDA, Washington DC

Rigon R, Bancheri M, Formetta G, de Lavenne A (2016) The geomorphological unit hydrograph from a historical-critical perspective. Earth Surf Proc Land 41(1):27–37. https://doi.org/10.1002/esp.3855

Rodríguez-Iturbe I, Devoto G, Valdés JB (1979) Discharge response analysis and hydrologic similarity: the interrelation between the geomorphologic IUH and the storm characteristics. Water Resour Res 15(6):1435–1444. https://doi.org/10.1029/WR015i006p01435

Sahoo R, Jain V (2018) Sensitivity of drainage morphometry based hydrological response (GIUH) of a river basin to the spatial resolution of DEM data. Comput Geosci 111(October 2017):78–86. https://doi.org/10.1016/j.cageo.2017.10.001

Sandeep P, Kumar KCA, Haritha S (2021) Risk modelling of soil erosion in semi-arid watershed of Tamil Nadu, India using RUSLE integrated with GIS and remote sensing. Environ Earth Sci 80(16):1–20. https://doi.org/10.1007/s12665-021-09800-6

Schumm SA (1956) Evolution of drainage systems and slopes In badlands at Perth Amboy, New Jersey. Bull Geol So Am 67(5):597–646

Shekar PR, Mathew A (2022) Prioritising sub-watersheds using morphometric analysis, principal component analysis, and land use/land cover analysis in the Kinnerasani River basin, India. H2Open J 5(3). https://doi.org/10.2166/h2oj.2022.017

Shelar RS, Shinde SP, Pande CB, Moharir KN, Orimoloye IR, Mishra AP, Varade AM (2022) Sub-watershed prioritization of Koyna river basin in India using multi criteria analytical hierarchical process, remote sensing and GIS techniques. Phys Chem Earth, Parts a/b/c 128(August):103219. https://doi.org/10.1016/j.pce.2022.103219

Singh S, Kansal ML (2020) Flash flood hazard mapping using satellite images and GIS: a case study of alaknanda river basin. In Flash floods: challenges and its management. The Institution of Engineers Centenary Publication, Kolkata, pp 77–83. https://www.ieindia.org/webui/ajax/Downloads/WebUI_PDF/Publication/Flash_Floods_Challenges_and_its_Management.pdf? v.20210212.1

Singh G, Chandra S, Babu R (1981) Soil loss and prediction research in India. Bulletin No. T-12/D9, Central Soil and Water Conservation Research Training Institute, Dehra Dun

Singh G, Rawat M, Pandey A (2023) Investigation of the flash flood event caused by a massive rock – ice avalanche in the Himalayan river valleys of Rishiganga and Dhauliganga , Uttarakhand. Nat Hazards 0123456789. https://doi.org/10.1007/s11069-023-05972-5

Singh S, Kansal ML (2022a) Chamoli flash-flood mapping and evaluation with a supervised classifier and NDWI thresholding using Sentinel-2 optical data in Google earth engine. Earth Sci Inf. https://doi.org/10.1007/s12145-022-00786-8

Singh S, Kansal ML (2022) Cloudburst—a major disaster in The Indian Himalayan states. In: Kolathayar S, Pal I, Chian SC, Mondal A (eds) Civil Engineering for Disaster Risk Reduction. Springer, Singapore, pp 115–126. https://doi.org/10.1007/978-981-16-5312-4_9

Singh S, Kansal ML (2023) Sub-basin prioritisation using RUSLE in a mountainous river basin of Uttarakhand (India). Environ Dev Sustain 0123456789:27. https://doi.org/10.1007/s10668-023-02989-5

Singh G, Pandey A (2021a) Evaluation of classification algorithms for land use land cover mapping in the snow-fed Alaknanda River basin of the Northwest Himalayan Region. Appl Geomat 13(4):863–875. https://doi.org/10.1007/s12518-021-00401-3

Singh G, Pandey A (2021b) Flash flood vulnerability assessment and zonation through an integrated approach in the Upper Ganga basin of the Northwest Himalayan region in Uttarakhand. Int J Disaster Risk Reduct 66(September):102573. https://doi.org/10.1016/j.ijdrr.2021.102573

Smith KG (1950) Standards for grading texture of erosional topography. In Am J Sci 248(9):655–668. https://doi.org/10.2475/ajs.248.9.655

Sofi MS, Rautela KS, Bhat SU, Rashid I, Kuniyal JC (2021) Application of geomorphometric approach for the estimation of hydro-sedimentological flows and cation weathering rate: towards understanding the sustainable land use policy for the Sindh basin, Kashmir Himalaya. Water Air Soil Pollut 232(7). https://doi.org/10.1007/s11270-021-05217-w

Sorman AU (1995) Estimation of peak discharge using GIUH model in Saudi Arabia. J Water Resour Plan Manag 121(4):287–293. https://doi.org/10.1061/(asce)0733-9496(1995)121:4(287)

Sridhar P, Ganapuram S (2021) Morphometric analysis using fuzzy analytical hierarchy process (FAHP) and geographic information systems (GIS) for the prioritization of watersheds. Arab J Geosci 14(4). https://doi.org/10.1007/s12517-021-06539-z

Srinivasan R, Karthika KS, Suputhra SA, Chandrakala M, Hegde R (2021) Mapping of Soil erosion and probability zones using remote sensing and GIS in arid part of South Deccan Plateau, India. J Indian Soc Remote Sens 5. https://doi.org/10.1007/s12524-021-01396-5

Strahler AN (1952) Dynamic basis of geomorphology. Paper Knowledge Toward a Media History of Documents 63(September):923–938. https://doi.org/10.1130/0016-7606

Strahler A (1964) Quantitative geomorphology of drainage basins and channel networks. In: Chow V (eds) Handbook of applied hydrology. McGraw Hill, New York, pp 439–476. https://cir.nii.ac.jp/crid/1572824500442828288

Sujatha ER, Sridhar V (2017) Mapping debris flow susceptibility using analytical network process in Kodaikkanal Hills, Tamil Nadu (India). J Earth Syst Sci 126(8). https://doi.org/10.1007/s12040-017-0899-7

Tesema TA (2022a) Erosion hotspot mapping using integrated morphometric parameters and land use/land cover of Jigjiga Watershed, Ethiopia. Heliyon 8(6):e09780. https://doi.org/10.1016/j.heliyon.2022.e09780

Tesema TA (2022b) Erosion hotspot mapping using integrated morphometric parameters and the land use/land cover of Jigjiga watershed, Ethiopia. Heliyon 8(April):e09780. https://doi.org/10.1016/j.heliyon.2022.e09780

Thakur PK, Dhote PR, Roy A, Aggarwal SP, Nikam BR, Garg V, Chouksey A, Pokhriyal N, Jani M, Chauhan V, Thakur N, Dogra VS, Rao GS, Chauhan P, Kumar AS (2020) Significance of remote sensing based precipitation and terrain information for improved

hydrological and hydrodynamic simulation in parts of Himalayan River basins. ISPRS - Int Arch Photogramm Remote Sens Spat Inform Sci XLIII-B 3–2:911–918. https://doi.org/10.5194/isprs-archives-xliii-b3-2020-911-2020
Tiwari RN, Kushwaha VK (2021) Watershed prioritization based on morphometric parameters and PCA technique: a case study of Deonar River sub basin, Sidhi area, Madhya Pradesh, India. J Geol Soc India 97(4):396–404. https://doi.org/10.1007/s12594-021-1697-z
Van der Knijff JM, Jones RJA, Montanarella L (2000) Soil erosion risk assessment in Europe. Luxembourg: Office for Official Publications of the European Communities, EUR 19022, 34. https://www.unisdr.org/files/1581_ereurnew2.pdf
Wischmeier WH, Smith DD (1978) Predicting rainfall erosion losses -a guide to conservation planning. Science and Education Administration. Department of Agriculture, Science and Education Administration, Washington, DC. https://books.google.co.in/books?hl=en&lr=&id=rRAUAAAAYAAJ&oi=fnd&pg=PA5&dq=Predicting+Rainfall+Erosion+Losses+-A+Guide+to+Conservation+Planning&ots=cvtvpWpm-Z&sig=LMDPXETL6AcZbIF_BbqqHNT77g&redir_esc=y#v=onepage&q&f=false
Yalcin A, Reis S, Aydinoglu AC, Yomralioglu T (2011) A GIS-based comparative study of frequency ratio, analytical hierarchy process, bivariate statistics and logistics regression methods for landslide susceptibility mapping in Trabzon, NE Turkey. Catena 85(3):274–287. https://doi.org/10.1016/j.catena.2011.01.014

Publisher's Note Springer Nature remains neutral with regard to jurisdictional claims in published maps and institutional affiliations.

Authors and Affiliations

Sachchidanand Singh[1,2] · Mitthan Lal Kansal[1]

Mitthan Lal Kansal
mlk@wr.iitr.ac.in

[1] Water Resources Development and Management, Indian Institute of Technology, Roorkee, Uttarakhand, India

[2] National Institute of Hydrology, Roorkee, Uttarakhand, India